Biogasoline Production from Waste Cooking Oil using Nano-Cobalt Molybdenum Catalyst

Kudzai Mabika (566462)

MSc 50/50 Research Report

1st June 2016

Declaration:

- I am aware that plagiarism (the use of someone else's work without their permission and/or without acknowledging the original source) is a criminal offense.
- I confirm that this work submitted for assessment is my own unaided work.
- I have followed the required conventions in referencing the thoughts and ideas of others.
- I understand that the University of the Witwatersrand may take disciplinary action against me if there is a belief that this is not my own unaided work or that I have failed to acknowledge the source of the ideas or words in my writing.

Signature: ……..

Kudzai Mabika

Acknowledgements

I would like to thank Chemical Industries and Education Authority (CHIETA) for funding my studies, without their financial assistance this work would not be possible.

I am forever grateful to my supervisor Dr D.B Nkazi, for his assistance in making this project a success and his continuous tireless efforts in his supervisory role. In addition, I would like to thank the School of Chemical and Metallurgical Engineering of the University of the Witwatersrand for use of their facilities and providing a good environment for my studies. To my colleagues and departmental staff, thank you for guidance and assistance in your various areas of expertise.

I would also like to acknowledge the school of chemistry and its staff for allowing me to use its resources for equipment construction and products analysis.

Lastly I would like to thank my family for their support in all my endeavours and for giving me the freedom and opportunity to pursue my dreams. To God be the glory for guidance and protection through all I do.

Abstract

The world is gradually shifting to renewable clean energy and away from fossil fuels which are considered to have a finite reserve and have negative impact on the environment. Many alternatives have been developed including biofuels. Of the biofuel family, not all products are produced at the same level given the differences in technological advancements. Commonly produced biofuels which are commercialised are bioethanol and biodiesel. Given that a large number of vehicles operate using gasoline, there is a need to develop biogasoline specific processes to produce biogasoline. Bioethanol is used as a blending agent and has a drawback of engine corrosion. Biogasoline can be used for blending or to substitute gasoline in existing motors. The main objective of the project was to produce biogasoline from waste cooking oil using nano-particle catalyst for better performance.

A Co-Mo/Al_2O_3 catalyst was synthesized and tested in two processes namely thermal cracking and hydrocracking. The waste cooking oil used in this study was pre-treated to remove salts and excess water prior to cracking process. Various analytical techniques were then used to characterize the catalyst, waste cooking oil and the products.

Waste cooking oil was successfully pre-treated for salt removal with salt dropping from 13.18% to 4.37%. Effect of catalyst performance on thermal cracking proved to be minimal with temperature being the major factor in cracking. The catalyst performed better under hydrocracking with effects of catalyst calcination temperature and catalyst/oil ratio being more apparent as opposed to thermal cracking. Highest percentage biogasoline achieved under thermal cracking was 81.6% at a reaction temperature of 600°C. The highest percentage biogasoline achieved under hydrocracking was 75.7% at a reaction temperature of 210°C, using calcined catalyst at 700°C, catalyst/oil mass ratio of 1/75 and reaction time of 1hr. The biogasoline produced had low sulphur content. The highest sulphur containing product for hydrocracking was 7.4% and that for thermal cracking was 1.3%.

It is recommended that the hydrocracking and thermal cracking methods be used for biogasoline production and that further research be done on the optimization of the biogasoline production process and synthesis of nano Co-Mo catalyst.

Contents

List of Tables

List of Figures

List of Abbreviations

Co	Cobalt
Mo	Molybdenum
Ni	Nickel
XRD	X-ray Diffraction
ICP-OES	Inductively Coupled Plasma Optical Emission Spectroscopy
GC-MS	Gas Chromatography Mass Spectroscopy
BET	Brunauer–Emmett–Teller
SEM	Scanning Electron Microscope
µm	micrometres
nm	nanometres
ml	millilitres
Å	Angstrom

Chapter 1. Research Background

1.1 Introduction

Petroleum provides about 40% of the world's energy requirements and nearly all of its transport fuels (Greene et al., 2006). It is widely acknowledged that oil reserves are a finite resource although new reserves are discovered and some tapped into every year. As a result of oil reserves being finite, much attention has been put into the research and production of alternate renewable sources of energy including biofuels. Biofuels are fuels derived from biomass for transportation or heating applications (Dufey, 2006). The time taken in producing biofuels dwarfs in comparison to the millions of years it takes for crude oil to be formed underground. Biofuels can then be blended with crude oil based fuels to reduce the strain and demand of crude oil fuels (McMillan, 1997). In addition, biofuels are regarded as environmentally friendly (Demirbas, 2009).

Raw material for biofuels is agricultural produce and much has been said about how this could compete with food supply and possibly lead to an increase in food costs (Hertel et al., 2010). Cost of feedstock oil is a problem with it costing up to 75% of production (Phan and Phan, 2008). However, used cooking oil offers an alternative route and can cost up to 2-3 times cheaper (Zhang et al., 2003). Waste cooking oil also deals with the concern of agricultural produce such as oils being used in activities other than human consumption in a world where food security is an issue.

Different methods are found in literature towards the processing of vegetable oils into biofuels but most are trans-esterification processes with a bias towards production of biodiesel. This paper takes a look at the hydro-processing and thermal cracking of waste cooking oil into fuel, with focus being on producing bio-gasoline whose methods are not at advanced stages as its biodiesel counterpart. The method of production is the hydrocracking process which is already vastly used in industry towards the upgrading of heavy oils (Mohanty et al., 1990). It combines feed stock oil and hydrogen at high temperatures and pressures over suitable catalyst to produce lighter oils such as diesel and gasoline. Focus is on the application of nano-sized Co-Mo catalyst towards achieving this goal with a close look at effects on parameter changes. The view is that through application of nano-sized catalyst,

higher yields due to increased surface area can be achieved and through manipulation of process parameters such as temperature and reaction time, selectivity can be pushed towards bio-gasoline production. The catalyst was also trialed in a thermal cracking environment which is an alternative process.

1.2. Problem Statement

Biogasoline is a potential renewable fuel of spark engine which can be used with or as a substitute for conventional crude oil based gasoline without changing the engine materials. Which biofuel production process and catalyst treatment should be used to produce higher biogasoline yield?

1.3. Aim and Objectives

The aim of this research is to investigate the production of biogasoline using nano-Cobalt Molybdenum based catalyst. To achieve this aim, the following objectives were studied:

- To synthesize a nano-Cobalt Molybdenum catalyst
- To investigate the effect of calcination on the activity of the catalyst;
- To measure effect of operating parameters towards bio-gasoline production in a batch hydrocracking system. Operating parameters include;
    1. Reaction temperature
    2. Calcination temperature
    3. Reaction time
    4. Oil/catalyst ratio
- To measure effect of operating parameters towards biogasoline production in a thermal cracking system. Operating parameters include;
    1. Reaction temperature
    2. Calcination temperature
    3. Oil/catalyst ratio
- To compare the bio-gasoline production in thermal cracking and hydrocracking systems.

Chapter 2. Literature Review

The motive behind biogasoline production is to have a substitute for traditional fossil fuels in light of the issue of fluctuating oil supply and negative environmental impacts. In order to gain a better understanding of the process, it is important to first discuss the current world fuel climate, which is the source of the motive; biofuels and how they fit into the fuel picture; how biofuels come into production and in particular biogasoline which is the target of this study. Attention will also be given to the types of reactions and catalysts used.

2.1 World Fuel Climate

The world is heavily dependent on fossil fuels for its energy demands and it is expected that by 2030 the world will still rely on fossil fuels for 84% of its energy demands (Shafiee and Topal, 2009). Fossil fuel encompasses all fuels found underground generated over millions of years. These include coal, gas and the all-important crude oil. Table 2.1 below shows estimates of world fossil fuel reserves as of the year 2006.

Table 2.1: World main fossil fuel reserves 2006 (Shafiee and Topal, 2009)

Region	Fossil fuel reserve (giga tonnes of oil equivalent)				Fossil fuel reserve (%)			
	Oil	Coal	Gas	Sum	Oil	Coal	Gas	Sum
North America	8	170	7	185	0.86	18.2	0.75	19.81
South America	15	13	6	34	1.61	1.39	0.64	3.64
Europe	2	40	5	47	0.21	4.28	0.54	5.03
Africa	16	34	13	63	1.71	3.64	1.39	6.75
Russia	18	152	52	222	1.93	16.27	5.57	23.77
Middle East	101	0	66	167	10.81	0	7.07	17.88
India	1	62	1	64	0.11	6.64	0.11	6.85
China	2	76	2	80	0.21	8.14	0.21	8.57
Australia and East Asia	2	60	10	72	0.21	6.42	1.07	7.71
Total	165	607	162	934	17.67	64.99	17.34	100

Although the above figures of fuel reserves are set to increase, the quantity of how much is available still remains unknown (Lior, 2008). According to Maugeri (2004), new discoveries only replace a fourth of what the world consumes. This gives rise to the need to find alternative fuel sources to ease the reliance on fossil fuels. In addition, table 1 shows that

certain regions of the world and certain countries have more reserves than others. Some have none at all. Given that the whole world is dependent on fossil fuels and not just specific regions, there is rise in dependency on the few fuel rich countries for energy. These countries tend to regulate prices with groups such as the Organization of the Petroleum Exporting Countries (OPEC) where none oil producing countries have no say (Hassan et al., 2015). An alternative fuel source for such countries would be ideal.

Over and above this, crude oil together with other fossil fuels poses a significant threat to the environment. Use of fossil fuels such as petroleum products lead to problems such as modifications in earth's surface layer, subsidence of ground surface after fuel extraction (Agarwal, 2007). The use of fossil fuels has led to increase in CO_2 levels in atmosphere from 280 PPM in pre-industrial era to 350 PPM now (Agarwal, 2007). CO_2 levels are rising with increase in fuel used, leading to greenhouse effect, acid rain, smog and climate change.

2.2 Biofuels

Biofuels are fuels derived from biomass for transportation and heating purposes (Dufey, 2006). Biomass covers a wide range of organic matter both plant and animal. Production of biofuels is one of the ways to supplement conventional energy sources and its popularity is gathering momentum. Table 2.2 shows the projection of biofuel demand.

Table 2.2: Transport sector biofuel consumption projection (Escobar et al., 2009)

	2004		2030	
	Demand (Mtoe)	% Highway transportation	Demand (Mtoe)	% Highway transportation
OCDE	8.9	0.9	84.2	7.2
North America	7	1.1	45.7	6.4
The USA	6.8	1.3	42.9	7.3
Europe	2	0.7	35.6	11.8
Pacific Islands	0	0	2.9	1.9
Transition economics	0	0	0.5	0.6
Developed Countries	6.5	1.5	62	6.9
China	0	0	13	4.5
India	0	0	4.5	8
Other Asian Developed Countries	0.1	0	21.5	4.6
Brazil	6.4	13.7	23	30.2
World	15.5	1	146.7	6.8
European Union	2	0.7	35.6	11.8

Biofuels provide a cleaner fuel source with lower concentrations in sulphur containing compounds which are harmful to the environment compared to conventional fuels (Escobar et al., 2009). Whether biofuels lower overall greenhouse gas emissions is still a topic of debate as life cycle analysis of biofuels are still being carried out. However if land use changes due to biofuel production are neglected, it is widely acknowledged that there is less greenhouse gases emitted as compared to when fossil fuels are used (Timilsina and Mevel, 2012). Another point of contention where biofuels are concerned is whether or not production of biofuels competes with food supply given that biofuel raw materials are mainly crops (Rosillo-Calle and Johnson, 2010). However, biofuels can be produced from waste material as is the case with biodiesel and bio-gasoline being produced from waste cooking oil and biogas being produced from sewage.

2.2.1 Biogas

Biogas is a gaseous product from the decomposition of organic matter (U.S Department of Energy, 2015 a). Anaerobic digestion of crops, residues and waste leads to the production of gas whose component of fuel value is methane (Weiland, 2009). This process readily makes use of abundant waste worldwide producing gas used in specialized cars, industry and for heating purposes. Much of the research for biogas lies within process optimization and adaptation to different feed stocks given that biogas production is already at a commercial stage like ethanol (Deublein and Steinhauser, 2011).

2.2.2 Biodiesel

Biodiesel is produced from vegetable oils, animal fats and used cooking oils. The main process that produces biodiesel is called trans-esterification. This process converts oils and fats into long-chain mono alkyl esters, which is biodiesel when used as a fuel, these chemicals are also referred to as fatty acid methyl esters (FAME) (U.S Department of Energy, 2014).

2.2.3 Bioethanol

Ethanol is the most common biofuel and is produced from fermentation of sugars. Figure 2.1 illustrates the stages involved in ethanol production.

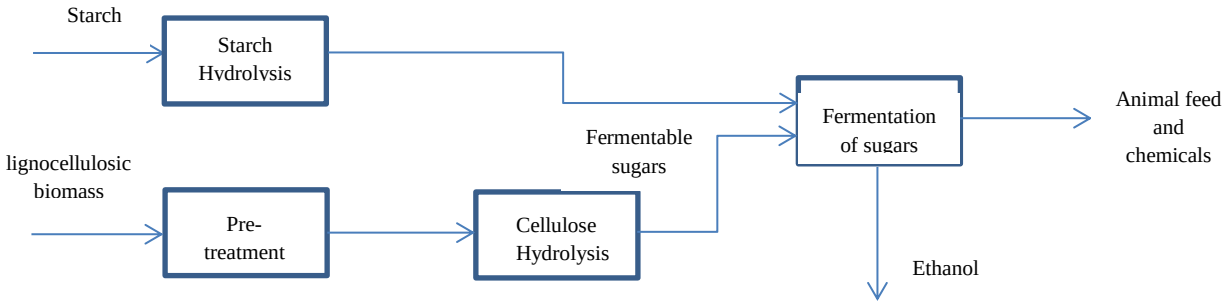

Figure 2.1: Ethanol production process (Gray et al., 2006)

Ethanol is commonly used for blending with conventional fossil fuel gasoline (Niven, 2005). Blending percentages have been known to range from 10% to as high as 85% with most modern cars able to operate on the mix without failure (U.S Department of Energy, 2015b). The blending of ethanol with fossil fuel gasoline effectively lowers pressure on the reserves of crude oil by supplementing towards its demand. It is anticipated that by 2025 Brazil, the largest ethanol producer would have replaced the world demand for gasoline by 5% through ethanol production (Cerqueira Leite et al., 2009). Ethanol however requires large land use to produce the crop necessary to make it and it has a lower heat of combustion than fossil fuel derived gasoline (Niven, 2005). There is therefore a need to come up with an alternative to overcome these difficulties. One such alternative is biogasoline.

2.2.4 Biogasoline

Production of biofuels is well documented in literature however that of bio-gasoline is not as advanced as that of ethanol, biogas or biodiesel all of which have years of being commercialised. This makes the study into biogasoline production highly relevant. Its

similarity to commercial gasoline makes it a more attractive blending agent or substitute as compared to other products such as ethanol. Biogasoline is advantageous because it is fully compatible with conventional gasoline, cars and present infrastructure (Hassan et al., 2015).

2.2.4.1 Biogasoline properties

Table 2.3 gives a summary of key components in biogasoline against European standards set for gasoline. The data further confirms that biogasoline is fully compatible with gasoline.

Table 2.3: Biogasoline properties and European Fuel Quality Directive 2009/30/EC and standard EN228:2008 (Aakko-Saksa et al., 2011)

	Biogasoline	**EN 228:2008**
Formula	C_4-C_{12}	
Molecular Weight g/mol	~ 60-150	
Density, kg/m^3	750	720-775
Octane number RON/MON	min 95/85	min 95/85
Reid vapour pressure, kPa	45-90	45-60/70
Distillation:		
Range, °C	30-210	
Final boiling point, °C	<210	max 210
Evaporated at 70°C, % v/v	20-48	20-48
Evaporated at 100°C, % v/v	46-71	46-71
Evaporated at 150°C, % v/v	> 75	min 75
Residue, % v/v	< 2	max 2
Energy content (LHV), MJ/kg	~ 43	
Energy content (HHV), MJ/kg	~ 45	
Flash point, °C	~40	

2.2.4.2 Review of biogasoline production processes

Various processes can be used in the production of biogasoline. Most of these processes are modifications to conventional processes in the petroleum industry such as fluid catalytic cracking FCC (Holmgren et al., 2007). Process variables such as temperature, pressure and

catalyst are changed so as to suit the biomass raw material as opposed to crude oil. Figure 2.2 summarises these processes.

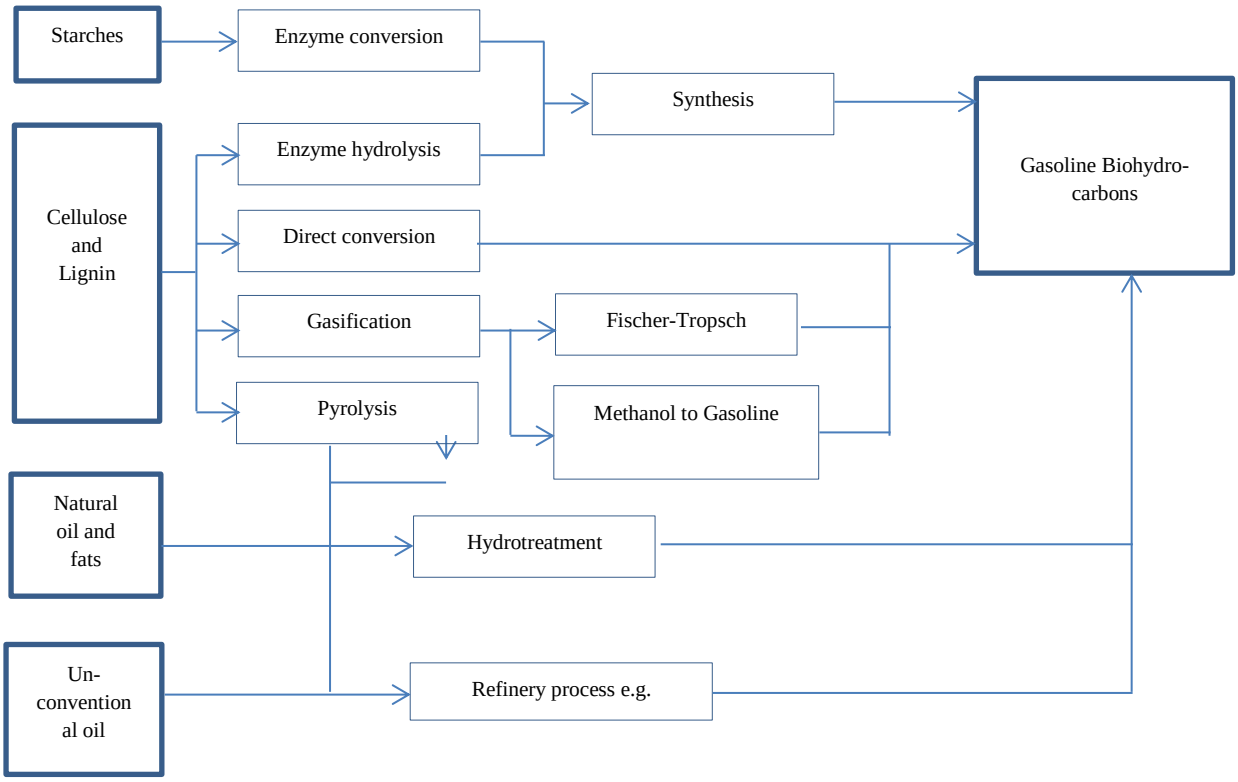

Figure 2.2: Biogasoline production processes (Huber et al., 2006)

In this study, the chosen feedstock is waste cooking oil (natural oil and fats) and the two processes are hydrotreatment (hydrocracking) and direct conversion via thermal cracking.

2.3 Cracking processes

In this study, two types of catalytic cracking were investigated for the production of biogasoline. The breakdown of hydrocarbons at higher temperature (termal cracking) and in the presence of hydrogen gas (hydrocracking).

2.3.1 Thermal Cracking

Thermal cracking is the breakdown of large hydrocarbon molecules into smaller chain hydrocarbons under high temperature and in the present of a catalyst (Vassiliou, 2009). This method has been widely used in the petroleum industry to refine crude oil to lighter products and its application has been stretched over to biofuel production.

The process usually takes place at high temperatures ranging from 600°C-850°C and at low pressure (Sadrameli, 2015). Feedstock ranges from crude oil and biomass in the case of biofuels.

The widely accepted theory to describe the cracking process is the Rice free radical theory explained through the cracking of paraffin (Greensfelder et al., 1949). Firstly, a paraffin molecule loses a hydrogen atom through collision and reaction with hydrocarbon radical and thereby turns into a radical. This radical may crack and become isomerized (change of position of Hydrogen atom). Cracking then occurs at the carbon – carbon bond forming an olefin and another radical. Radicals then crack and react with fresh feed and the chain reaction continues (Greensfelder et al., 1949).

2.3.2 Hydrocracking

Hydrocracking is the process by which hydrocarbons are broken down under low temperature and pressure over a suitable catalyst in the presence of hydrogen to produce shorter chain molecules (Tiwari et al., 2011). Shorter chain molecules are the various petroleum products. The waste cooking oil contains fatty acids which are the targeted long carbon chains. The wide range of products that arise from hydrocracking make it difficult to specify the reactions that take place (Mohanty et al., 1990). Variation in feedstock, catalyst, reactor configuration and reaction conditions add to the variation in possible products that can be attained. Authors have come up with different models for the kinetics and reaction mechanism that take place for each given combination of conditions.

For the proposed feedstock that will be used and reaction conditions, the model proposed by Botchwey et al., (2004) is assumed to best describe the reaction process. To come up with the

model, $NiMo/Al_2O_3$ catalyst was used in a trickle bed reactor under similar condition ranges that will be applied in the experiments to follow. The figure below outlines this mechanism where solid lines indicate hydrocracking processes and dotted lines indicate cracking reactions.

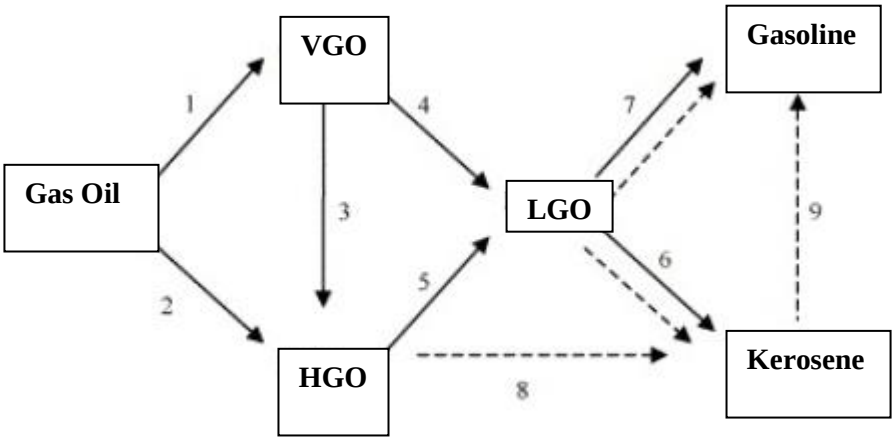

Figure 2.3: Reaction network proposed by Botchwey et al., (2004)

2.4 Catalysts used in cracking process

The type of catalyst used varies with the feedstock being used and the desired product (Mohanty et al., 1990). With hydrocracking, the catalyst plays a double function, firstly by acting as an active site for cracking the fatty acid molecules and then by acting as an active site for the addition of hydrogen atoms to the chain. Table 2.4 below shows various catalysts that have been used and the yield of bio-gasoline that has been obtained through hydrocracking.

Table 2.4: Catalysts used for hydrocracking and their yields

Feedstock	Catalyst	Bio-gasoline Yield (%)	Author
Fresh cooking oil	Commercial catalyst	10	(Bezergianni et al., 2009)
Used cooking oil	Commercial catalyst	8	(Bezergianni and Kalogianni, 2009)
Calophyllum inophyllum oil	Co-Mo/γ-Al_2O_3	25.63	(Rasyid et al., 2015)
Calophyllum inophyllum oil	Co-Mo/SiO_2	1.11	(Rasyid et al., 2015)
Calophyllum inophyllum oil	Co-Mo/γ-Al_2O_3-SiO_2	-	(Rasyid et al., 2015)
Vacuum gas oil	β+ASA/Ni-Mo	23.4	(Ali et al., 2002)

From the table it can be seen that bio-gasoline yield is low and waste cooking oil is rarely used as a feedstock. It is desired to obtain a high bio-gasoline yield from waste cooking oil. The proposed catalyst is a Co-Mo/γ-Al_2O_3 similar to the one used by Raysid et al., (2015) however an attempt will be made to synthesize a nano-catalyst.

Chapter 3: Experimental procedures and analysis techniques

Laboratory work fell under five key areas. These were waste cooking oil pre-treatment, catalyst synthesis, thermal cracking, hydrocracking and product and catalyst characterization. These are outlined in the following sections.

3.1 Waste cooking oil pre-treatment

The waste cooking oil is known to contain impurities commonly salt, food particles and water which are all introduced when cooking and frying. It is necessary to remove these impurities as they hinder catalyst performance through blocking active sites and taking part in some of the reaction (Forzatti and Lietti, 1999). This could lead to undesired product and poor yield.

The waste cooking oil was filtered to remove solid particles using a sieve of mesh size 50 µm. To remove salt, excess water was added (1 liter of water for every 500 milliliters of oil) and the mixture shaken vigorously in a closed flask. Salt dissolves in water and thus moves from the oil phase to the aqueous phase. The flask was left to stand for 24hrs before decanting. The oil phase was then heated in a silicon oil bath above 100°C for a period of 30 minutes to remove any remaining water. Figure 3.1 outlines the treatment process.

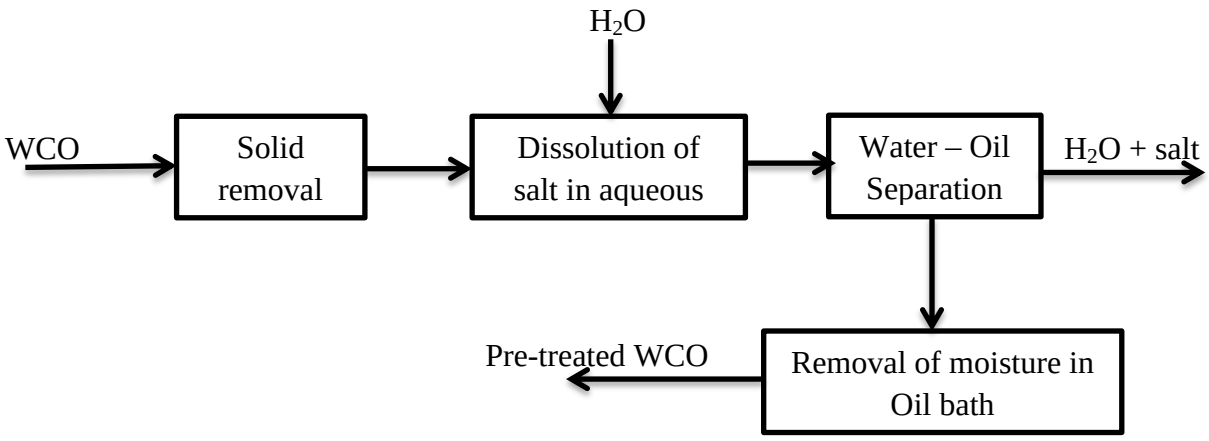

Figure 3.1 Waste cooking oil pre-treatment process

3.2 Catalyst Preparation

The catalyst prepared was a Cobalt-Molybdenum supported on Aluminium Oxide powder. The method of synthesis was an impregnation process of the aluminium oxide with a solution made up of dissolved cobalt and molybdenum salts (Choi et al., 2004).

Two salts, ammonium molybdate tetrahydrate [$(NH_4)_6Mo_7O_{24}\cdot 4H_2O$] and cobalt nitrate hexahydrate [$Co(NO_3)_2\cdot 6H_2O$] were weighed in varying mole ratios (1:1, 1:2, 1:3, 2:1, 3:1) and dissolved in an acidic pH 2 solution. After dissolving, each different mole ratio sample solution was added to aluminium oxide (Al_2O_3) powder of particle size ranging 63-200µm to give five different catalyst slurries. The amount of solution used to impregnate the support (Al_2O_3) was estimated as the voidage volume of the dry support powder. The voidage volume was estimated using the equation given below. Given that impregnation is about adding just enough to wet the support, this volume was considered sufficient. 10g of AL_2O_3 had a voidage volume of 7.5ml which was the amount of solution added. The slurries were then dried in an oven 24 hours at 120°C to remove water. The samples were then calcined in a furnace at a temperature of 600°C for 4 hours.

$$Voidage\ volume = measured\ Al_2O_3\ volume - (Al_2O_3\ measured\ mass / Al_2O_3\ density) \qquad \text{Equation 1}$$

Characterization of the catalyst was then used to determine which metal mole ratio (Co:Mo) was best. The best mole ratio was then used to produce catalyst which was calcined at varying temperatures (300°C, 400°C, 500°C, 600°C and 700°C).

All catalyst samples were stored in a desiccator to protect the catalyst from moisture exposure. Moisture exposure could lead to catalyst deactivation as it reacts with SO_3 (sulphur trioxide) in the catalyst producing sulphuric acid leading to deformation and degradation (Leach, 1983).

3.3 Thermal Cracking

Thermal cracking was carried out in a tube furnace. Treated waste cooking oil was mixed in a vial with catalyst in a mass ratio of 1:75 (catalyst: oil) (Mohammad Nasikin et al., 2009). The mixture was then emptied into a glass boat and placed in a glass tube in a tube furnace. The tube furnace temperature was then set and the experiment run with nitrogen gas being supplied into the system to carry off gaseous products to the product collection flask. The flask where the product was collected was kept in an ice bath to cool and condense the products which on leaving the vessel were vapours. This is essential as uncondensed vapour was vented out of the laboratory to avoid gas build-up. It is expected that the product of interest biogasoline condenses in a 0°C ice bath. This is based on the estimate for commercial gasoline which boils in the range 30°C-220°C (Government of Canada, n.d.). Figure 3.2 shows the experimental setup.

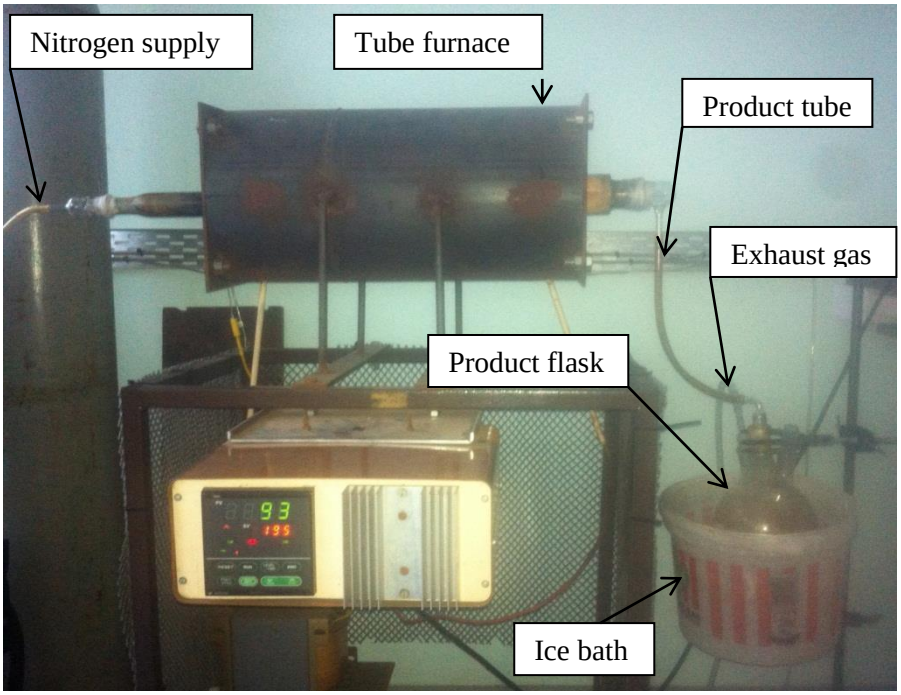

Figure 3.2: Thermal cracking setup

Care was taken to make sure that the system was sealed to avoid any gas leaks. Furnace temperature, catalyst ratio and calcination temperature of catalyst were the variables for this experiment.

3.4 Hydrocracking

195ml of treated waste oil was mixed with 2.6g Co-Mo/Al_2O_3 catalyst (Botchwey et al, 2004) and was poured into a three neck round bottom flask as shown in Figure. 3.3.

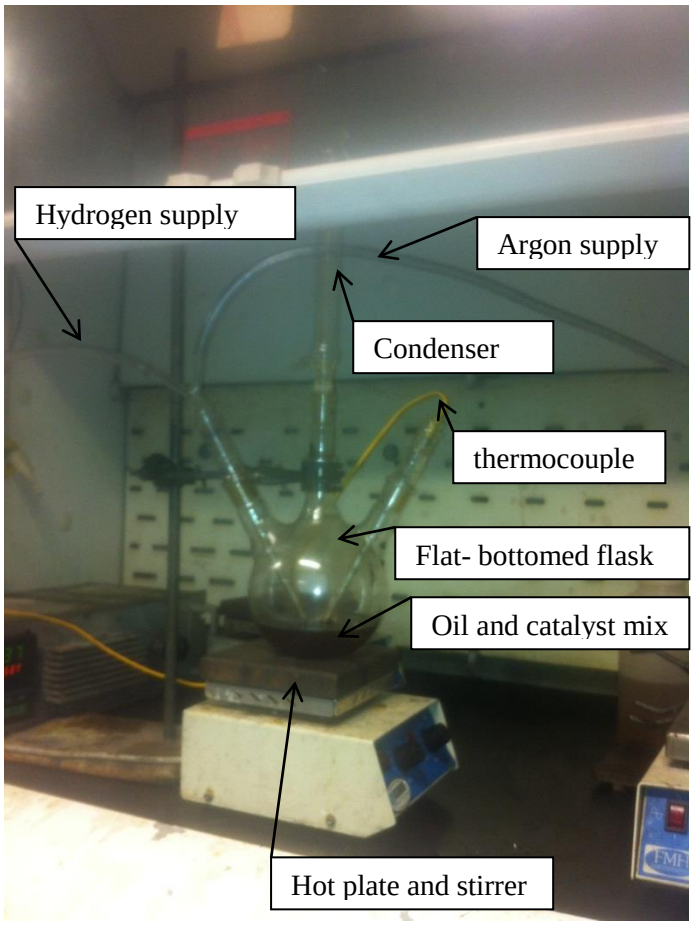

Figure 3.3: Hydrocracking setup

The batch experiment was run at varying reaction temperature, catalyst calcination temperature, reaction time and catalyst/oil ratio. Care was taken to ensure that before each run, the system was flushed with argon gas for a minute to clear it of air, Air and the reactant hydrogen form an explosive mixture. Throughout each run, argon gas was supplied in excess of the reactant hydrogen in order to promote an inert atmosphere in the vessel. Hydrogen gas was supplied directly into the liquid oil. Work was done in a fume hood to avoid gas build-up in the lab. The mixture was continuously stirred to promote mass transfer and reaction kinetics while the hot plate used for mixing and stirring was first calibrated with test runs to

ensure good temperature control. In addition, a reflux system was used to condense volatile hydrocarbons.

3.5 Analytical Techniques

The following techniques were used to analyse the catalyst:

- X ray Diffraction (XRD) – Compositional analysis
- Inductively Coupled Plasma Optical Emission Spectroscopy (ICP-OES) – Elemental concentrations
- Scanning Electron Microscope (SEM) – Morphology
- Brunauer–Emmett–Teller (BET) – Pore size and Diameter

The following techniques were used to analyse the waste cooking oil and subsequent product:

- Gas Chromatography Mass Spectroscopy (GC-MS) – Composition
- Volume and Mass measurements – Density

3.5.1 XRD

X-ray diffraction was used to identify the crystallinity of the catalyst and identify the phases present of the metals in the sample. A Bruker D2 Phaser was used for the analysis. Conditions were room temperature and atmospheric pressure, Cobalt radiation at a wavelength of 1.789997Å. The analysis run time was 10 minutes. The method is a non-destructive method as the sample is retained.

3.5.2 ICP-OES

This analysis was used to determine the Cobalt and Molybdenum concentration in the samples. 0.5 grams of each catalyst sample of varying Co/Mo ratio was mixed with 8ml nitric acid and 2ml sulphuric acid and was digested in a microwave reaction system Microwave 3000® at a maximum pressure of 31 bars for 40 minutes each. After this the liquid samples

were analysed using an ICP-OES Spectro Genesis having three runs for each sample which were then averaged for accuracy.

3.5.3 SEM

1g of each catalyst samples were mounted onto sample holders using Polyfast resin. A FEI Quanta 200 ESEM was then used for the sample imaging.

3.5.4 BET

0.2g of each catalyst sample was degased under Nitrogen for 12hrs at 120°C to remove any moisture. A Micromeritics Tristar 3000 was then used to obtain surface area, pore volume and pore size data.

3.5.5 GC-MS

The waste cooking oil and the product from all the reactions were analysed using a LECO Pegasus 4D GC in combination with an Agilent Technologies 7890B mass spectrometer. For each sample, 1µL of sample was injected with helium as the carrier gas through the column at a maximum temperature setting of 350°C. This analysis allowed for the identification of all compounds in the samples.

Chapter 4: Results and Discussion

This section looks to explain and give an in depth analysis of the experimental work and where possible give comparison to work done in literature. The results are for the catalyst synthesis, oil treatment and bio-gasoline production.

4.1 Catalyst Characterization

The catalyst went under four different characterization techniques which sought to identify the size, morphology and composition of the catalyst. These are discussed in the sections below.

4.1.1 ICP-OES analysis

This technique was used specifically for determining the Cobalt to Molybdenum mole ratio in the sample. The desired ratio was 1:1 as suggested by Choi et al., (2004). The results of the five catalyst samples that were analysed are shown in table 4.1.

Table 4.1: Catalyst metal mole ratio determination

Expected ratio on mixing	Moles in sample as per ICP-OES analysis		Calculated ratio as per ICP-OES analysis	% Error
	Cobalt	Molybdenum		
1:1	0.1099	0.1108	1:0.992	0.80
1:2	0.1474	0.3002	1:2.037	-1.85
1:3	0.0012	0.0041	1:3.31	-10.33
2:1	0.3053	0.1638	1.864:1	6.80
3:1	0.5142	0.2022	2.543:1	15.23

The results of the ICP-OES analysis show that catalyst mixing was accurate given the low percentage error. It was then decided to continue catalyst production with the salt solution that was used to make the 1:1 sample as it had a low percentage error of 0.8% and fell close to the 1:1 ratio suggested by literature.

4.1.2 XRD analysis

XRD analysis was performed on the $CoMo/Al_2O_3$ catalyst to observe crystallinity and phases present. Two sets of catalyst were run through the XRD, these were the catalyst with varying mole ratio of metal ions and the catalyst with varying calcination temperatures.

For the variation in metal ion ratio, figure 4.1 shows that on a 2 theta scale, all five samples produced similar graphs, with peaks in the same positions. This trend can be attributed to the fact that XRD is a qualitative analysis and in so being, does not pick out the variations in metal ion concentrations in the sample. It is because of this reason, that ICP-OES analysis was conducted.

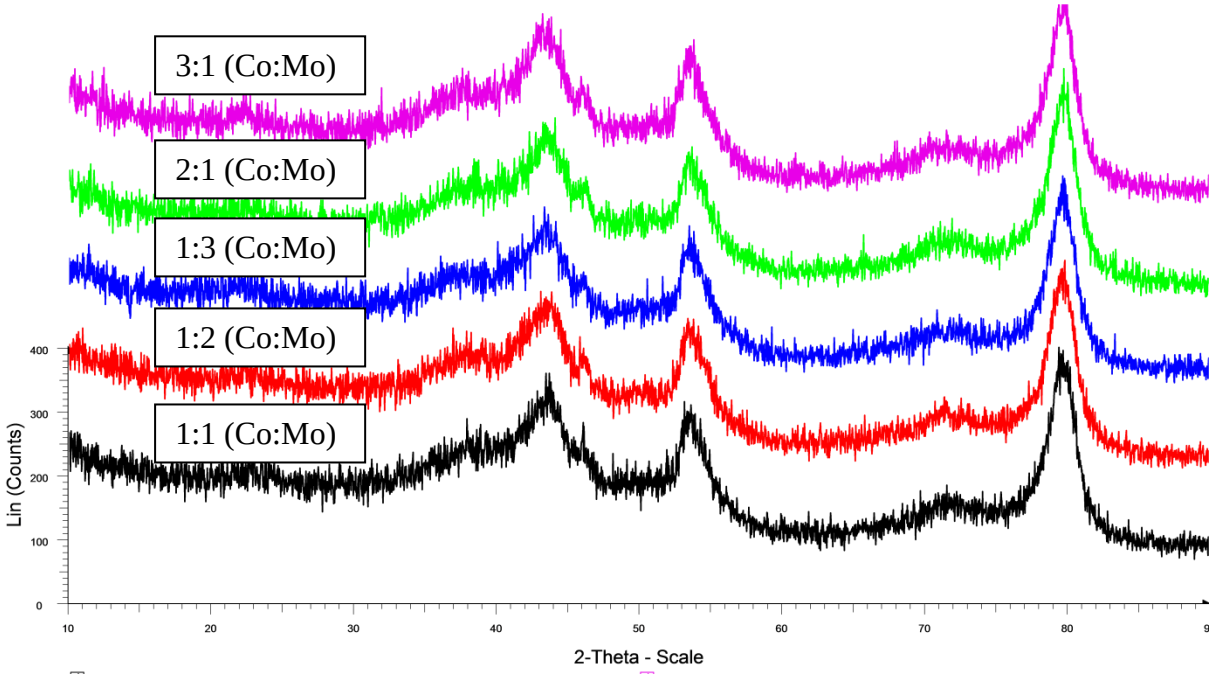

Figure 4.1: XRD graphs for varying metal ion concentrations

A closer look at a single graph is given below and it shows the different complexes that resulted in major peaks on the 2 theta XRD analysis.

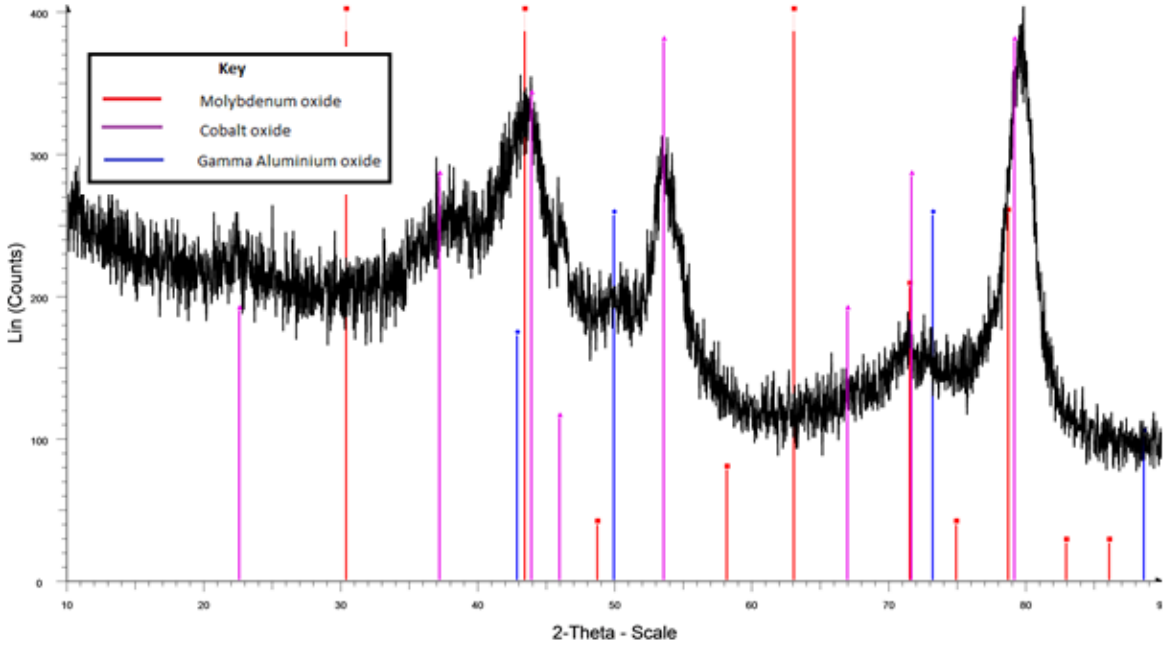

Figure 4.2: XRD graph for catalyst ratio showing complexes present

The graph shows that Molybdenum oxide, cobalt oxide and gamma aluminium oxide were present in the sample. This served as confirmation that the required constituencies of the catalyst were present.

Furthermore, the XRD graph obtained is similar to the one found in literature of the same catalyst which was synthesised by Rasyid et al., (2015). The comparison between the two graphs is shown in figure 4.3

a) b)

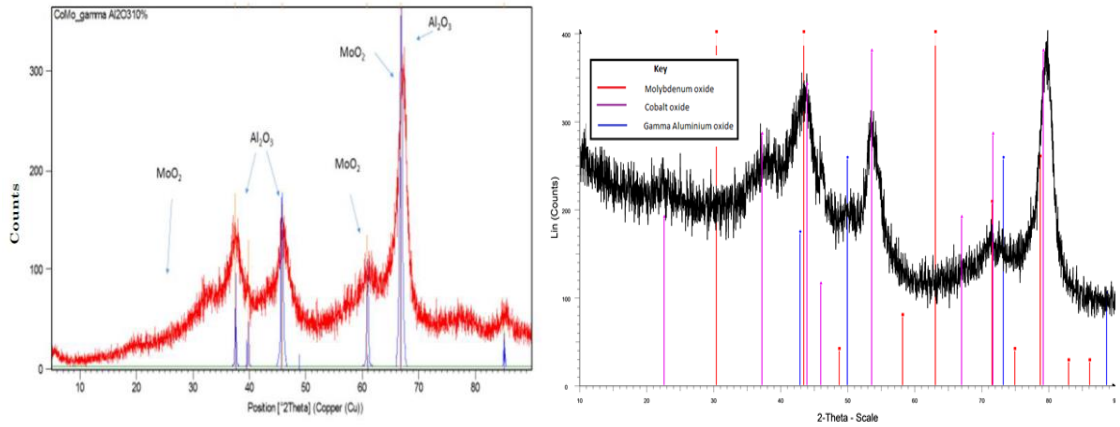

Figure 4.3: a) CoMo/Al_2O_3 XRD graph (Rasyid et al., 2015) b) XRD graph obtained for synthesised catalyst

The second set of XRD analysis focused on the differences of the samples as calcination temperature changed. Figure 4.4 shows the five graphs of the five catalyst samples calcined at different temperatures.

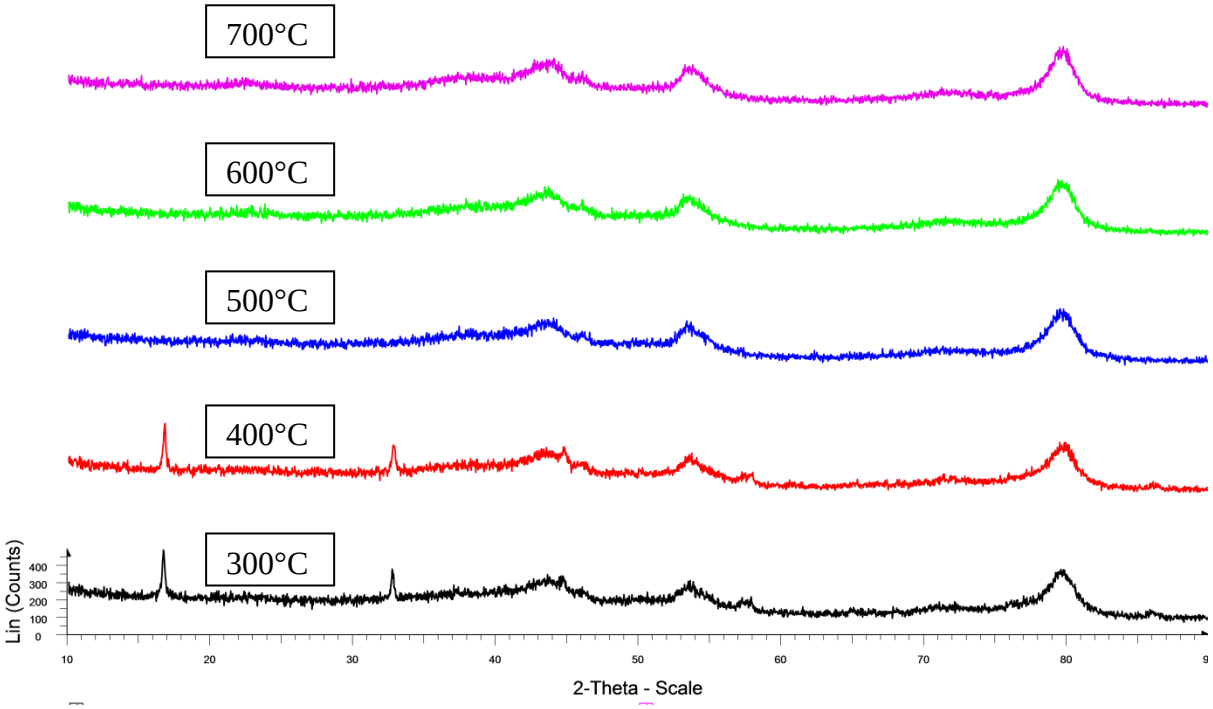

Figure 4.4: $CoMo/Al_2O_3$ XRD graphs for varying calcination temperatures

The graphs for 500°C, 600°C and 700°C were similar and their trends are the same as those outlined above in figure4.4. Graphs for 300°C and 400°C produced extra peaks at lower angles. Figure 4.5 focuses on complexes present for 300°C and the 400°C samples.

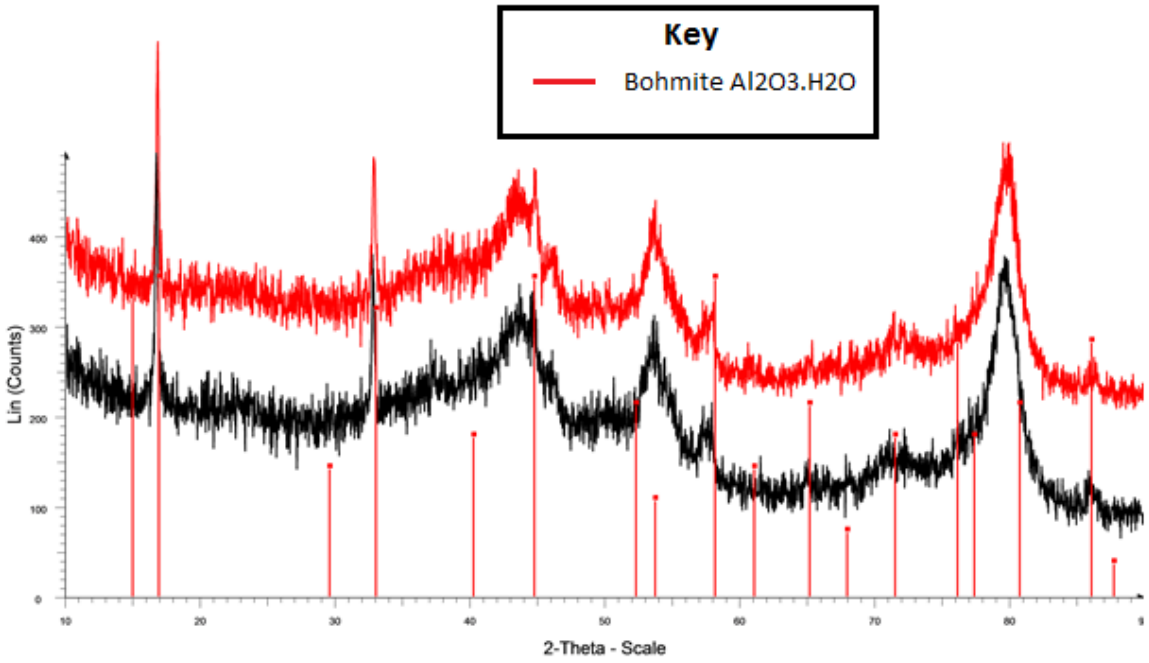

Figure 4.5: $CoMo/Al_2O_3$ graphs for 300°C and 400°C

The extra peaks on the graphs at 300°C and 400°C are as a result of the presence of Bohmite. This is an aluminium oxide hydroxide complex, crystalline in nature. It is bulky in nature and is present as a result of incomplete dehydration of the catalyst which is typical at low calcination temperatures. This suggests the need to use a catalyst calcined at higher temperatures (500°C and above). Complexes such as bohmite lower catalyst activity which can lead to lower yields and inefficient cracking in the production stages.

4.1.3 BET analysis

Brunauer–Emmett–Teller analysis provided information on the textual properties of the catalyst. The method is a function of gas adsorption onto the sample surface. Table 4.2 gives the properties that were observed for the five samples which had different calcination temperatures.

Table 4.2: BET $CoMo/Al_2O_3$ catalyst textual properties for different calcination temperatures

Calcination temperature (°C)	BET surface area (m^2/g)	Pore volume (cm^3/g)	Pore size (nm)
300	158.0640	0.210678	5.33145
400	169.0324	0.226162	5.35192
500	162.1202	0.240432	5.93219
600	129.5474	0.224126	6.92027
700	122.2886	0.239808	7.84402

From the data it can be seen that change in calcination temperature did not have a notable impact on the pore volume therefore the main points are the variation in surface area and pore size. Figure 4.6 shows that the surface area increased with increase in calcination temperature and peaked at 400°C with a surface area of 169.032 m^2/g. It then decreased gradually to a surface area of 122.29m^2/g.

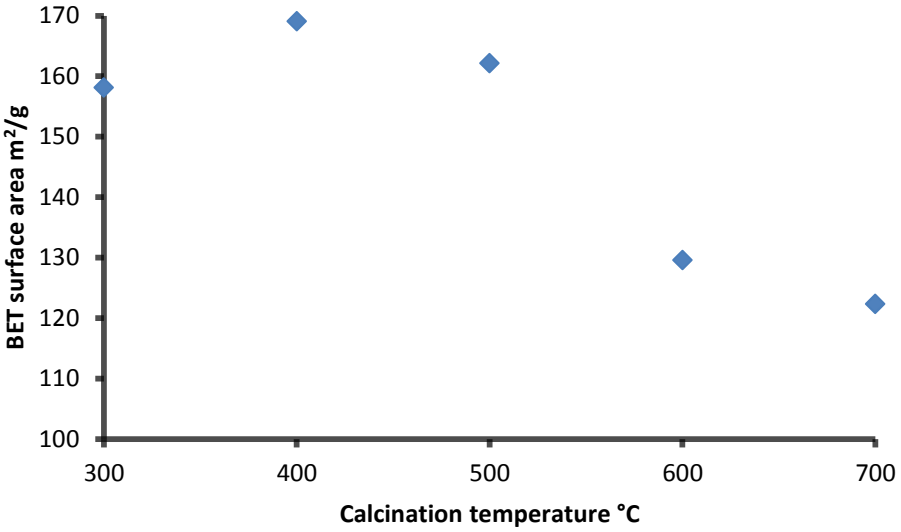

Figure 4.6: Catalyst surface area variation with calcination temperature

Generally increase in calcination temperature leads to a decrease in surface area. This is synonymous with the work done by Al-Fatesh and Fakeeha (2012) and Xiong et al., (2005). Both noted a decrease in surface area with an increase in calcination temperature for their Ni/Al_2O_3 and Co/Al_2O_3 catalysts respectively. This drop in surface area can be attributed to increased agglomeration and sintering of catalyst particles at higher temperatures (Gaber et al., 2016). As the particles agglomerate, the surface area which was once exposed is no longer available thereby leading to a reduction. With regards to the pore size, the size increases with an increase in calcination temperature peaking at 7.84nm for 700°C from an initial 5.33nm at 300°C as shown in figure 4.7.

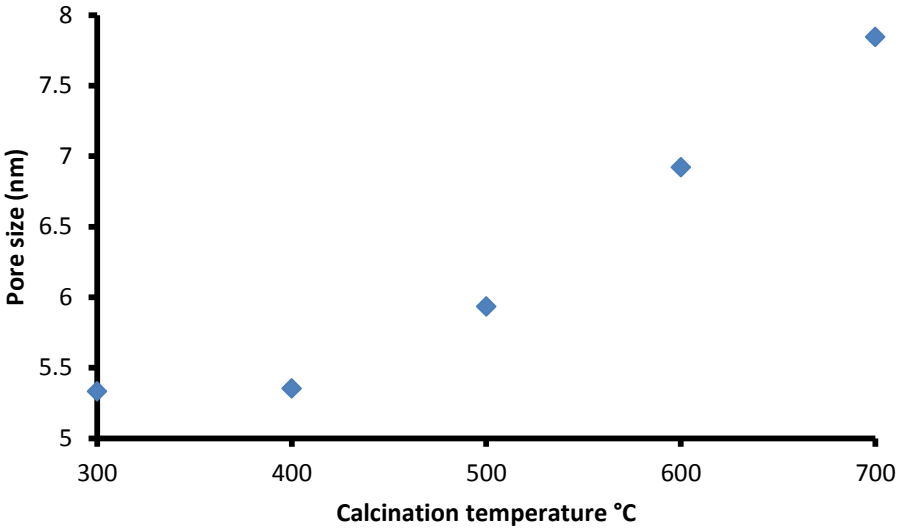

Figure4.7: Change in pore size with calcination temperature

This again is similar to the trends observed by both Al-Fatesh and Fakeeha (2012) and Xiong et al., (2005) with regards to pore size change. The reason for an increase in pore size is similar to the one for decrease in surface area. Agglomeration of particles leads to creation of bigger spaces between the particles, which translate to an increase in pore size. It is important to note that the pore size is of nano-scale therefore it can be said that the catalyst and the reactions that take place will be at this scale. Nano-scale is the target for the catalyst in this research.

While it is desired to have a catalyst with higher surface area for an increased amount of collisions of reactants on the catalyst active site, the pore size also plays a vital role. A bigger pore volume encourages good mass transfer for the reactants to be carried to the active sites and products away from the catalyst active sites (Roberts, 2008). Given that one when is increasing the other is decreasing as calcination temperature changes, it was decided that all calcination temperatures be trialled in the bio-gasoline production to ascertain which is a better catalyst.

4.1.4 SEM analysis

At low magnifications, the SEM images for all the catalyst samples looked similar. One such image is shown in figure 4.8. For more low magnification images please refer to appendix A.

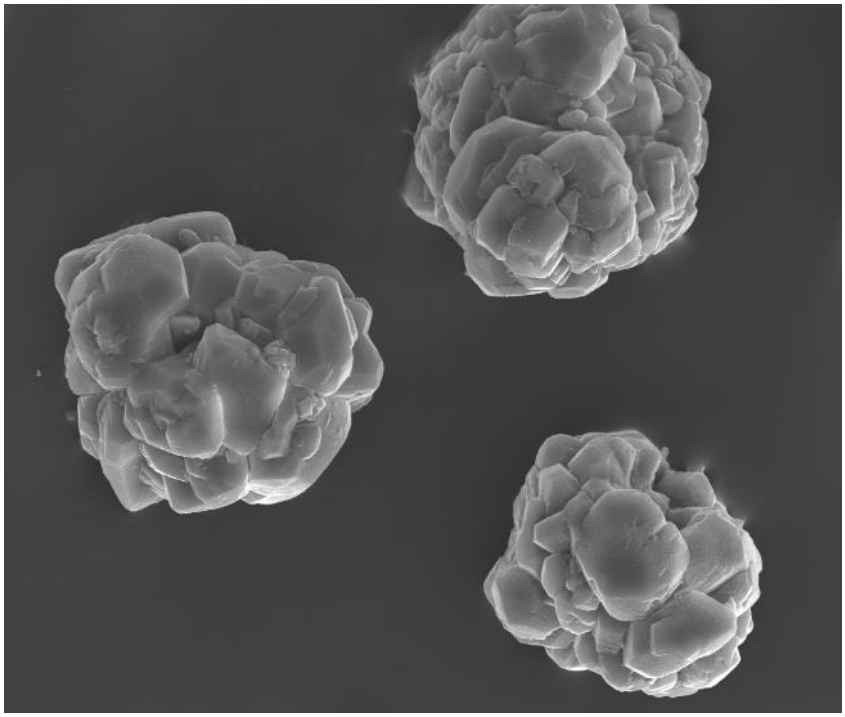

Figure 4.8: Low magnification image of $CoMo/Al_2O_3$

High magnification images of the catalyst show that as calcination temperature increases, the there is a notable change in the texture of the catalyst and there are smaller catalyst particles present at nano scale as shown in figure 4.9.

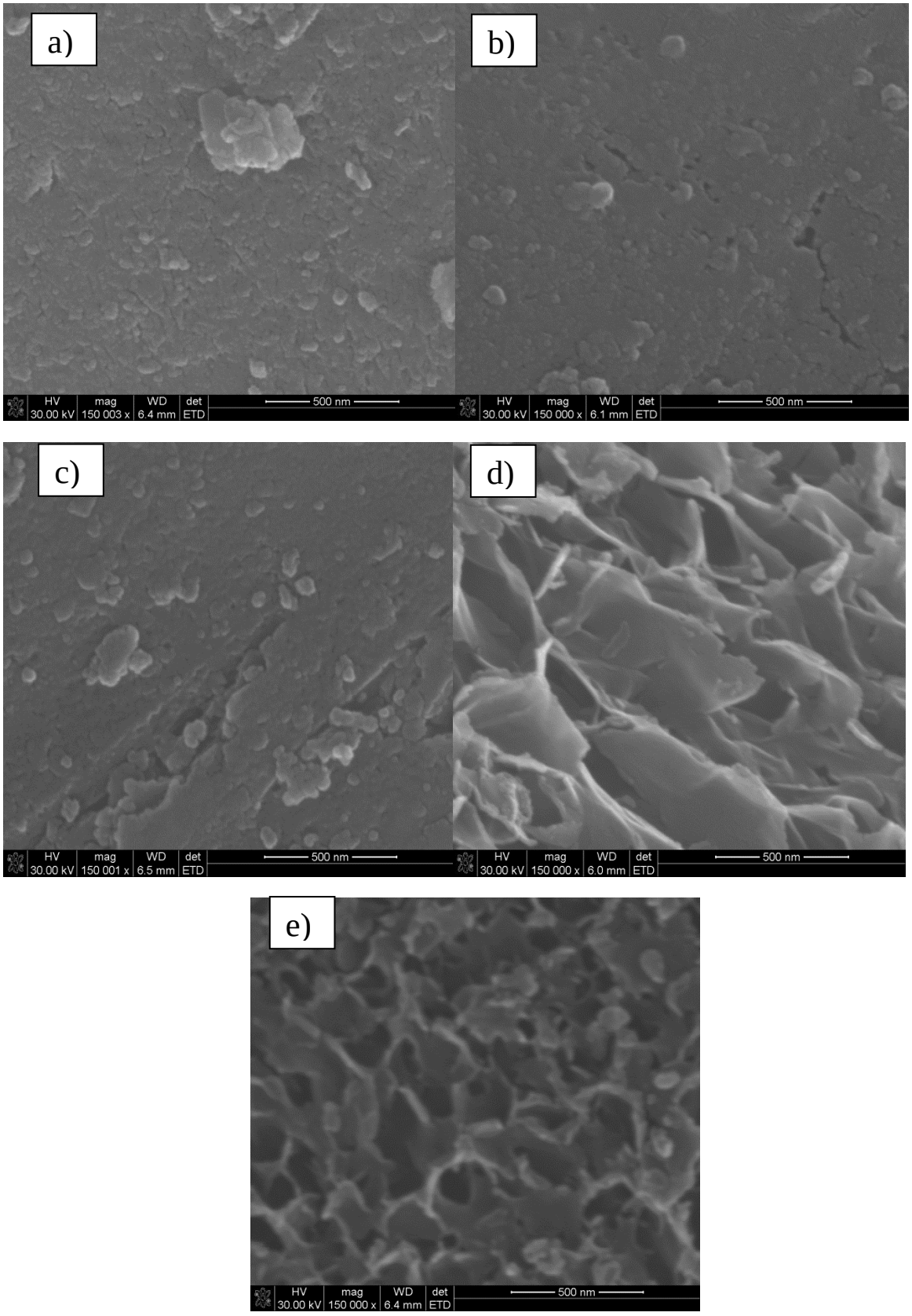

Figure 4.9: SEM images for varying calcination temperatures a) 300°C b) 400°C c) 500°C d) 600°C e) 700°C

The SEM images show that as calcination temperature increases, there is an increase in the breakage of the catalyst and development of pits on the catalyst surface. This can be attributed to the increase in heat which is breaking up the catalyst. This is an advantage as it makes the catalyst more accessible to raw materials leading to higher reaction rates.

4.2 Oil Pre-Treatment

Initially the waste cooking oil was cloudy and had solid particles in it. After treatment, it became clearer as a result of the solids and water removal. The oil before and after it was treated is shown in figure 4.10.

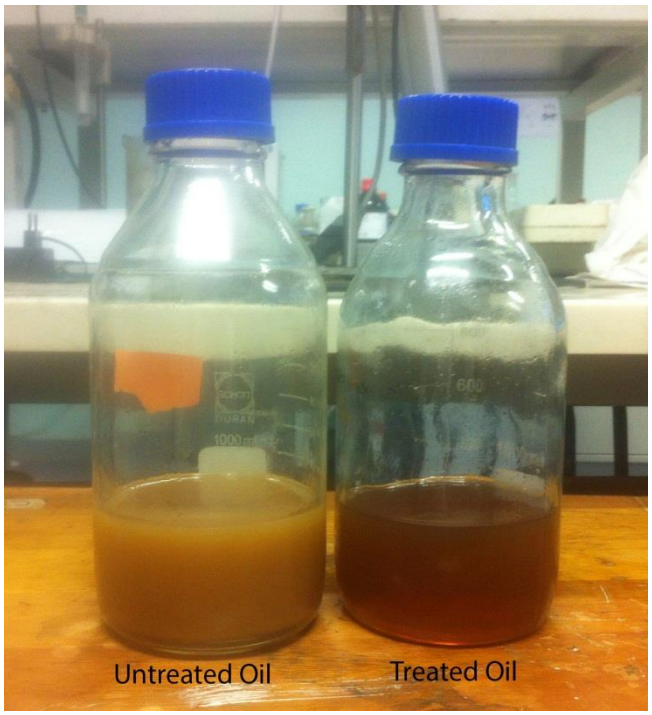

Figure 4.10: Waste cooking oil before and after treatment

The two oil samples were run through GC-MS to analyse the change after treatment and the following TIC images were obtained.

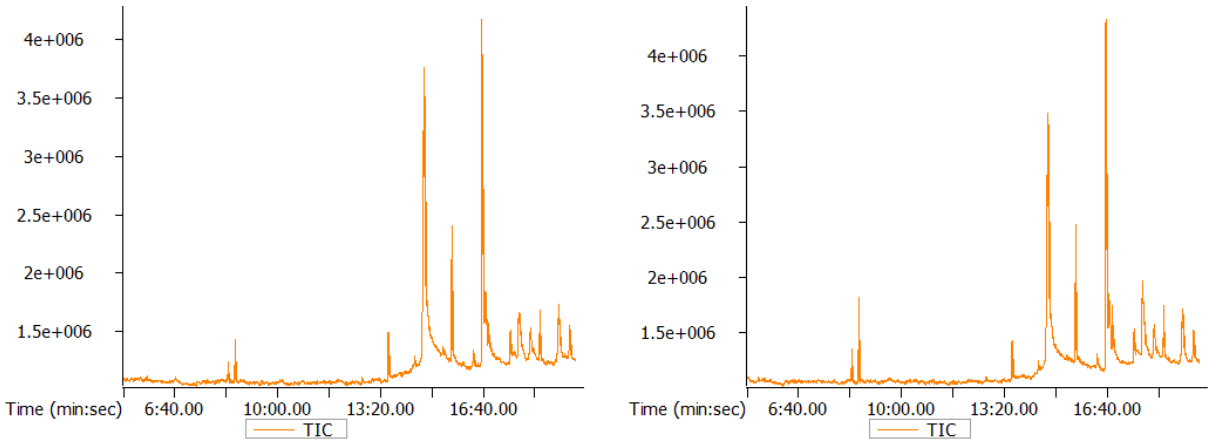

Figure 4.11: TIC images for a) untreated oil b) treated oil

The treated and untreated oils produced similar peaks as seen in figure 4.11 above however, analysis of compounds present in the oils shows a reduction in chloride, bromide and fluoride containing compounds. All of which are commonly associated with salts which are targeted for removal in the treatment process. These compounds accounted for 13.18% of the untreated oil as compared to 4.37% in the treated oil. This is an indication of salt removal from the oil as the salt dissolved in the water during the pre-treatment process. The presence of salts within the system could lead to salt crystallization which in turn can close catalyst pores during reaction and lower the available surface area thus leading to reduced catalyst activity (Lantelme and Groult, 2013).

4.3 Thermal cracking

Thermal cracking was conducted on the oil with the $CoMo/Al_2O_3$ catalyst. The three variables were catalyst calcination temperature, oil/catalyst ratio and reaction temperature and the results of the products are discussed below.

4.3.1 Catalyst calcination temperature variation

The calcination temperature of the catalyst was varied whilst reaction time (1.5hrs), reaction temperature (450°C) and catalyst/oil ratio (1/75) were kept constant. Figure 4.12 shows the trend as the calcination temperature changes.

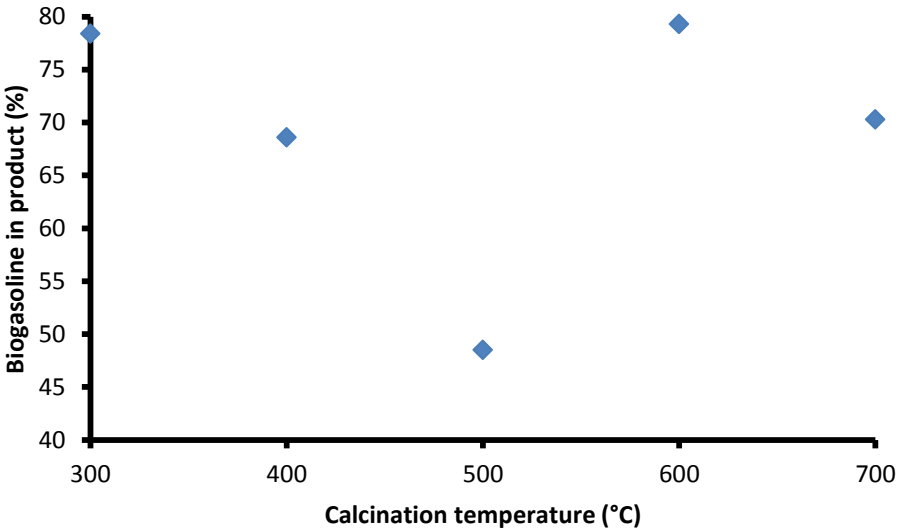

Figure 4.12: Change in bio-gasoline with calcination temperature

The results suggest that variation in calcination temperature has an ieffect on the production of biogasoline as there is no distinct trend that can be observed. This suggests that other parameters could have an impact on the cracking of the oil and would need to be analysed.

4.3.2 Oil/catalyst ratio variation

The oil/catalyst weight ratio was varied holding reaction temperature at a constant 450°C, calcination temperature at 700°C and reaction time at 1.5hrs. The amount of biogasoline in the products was within 1% of each other for runs done without catalyst, half catalyst and doubles the suggested weight given by Mohammad Nasikin et al., (2009). The highest biogasoline yield was obtained using the suggested literature value of 1:75 for catalyst to oil ratio with a value of 67.8% as shown in figure 4.13.

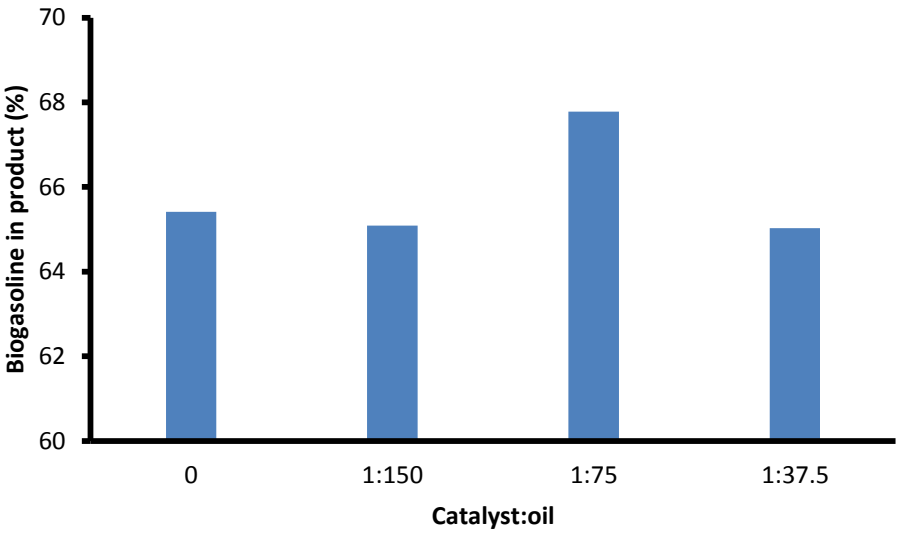

Figure 4.13 Change in bio-gasoline with catalyst oil ratio

From these results it is noted that a change in catalyst amount had minimal effect on the biogasoline produced as the difference between the highest and the lowest was 3%. This suggests that other parameters have an effect on the production.

4.3.3 Reaction temperature variation

Reaction temperature was varied while the catalyst/oil ratio, calcination temperature and the reaction time were kept constant at 1/75, 700°C and 1.5hrs respectively. Biogasoline in product increased with an increase in temperature and peaked at 600°C with 82% of the product being biogasoline. At higher temperatures, the biogasoline reduced as shown in figure 4.14.

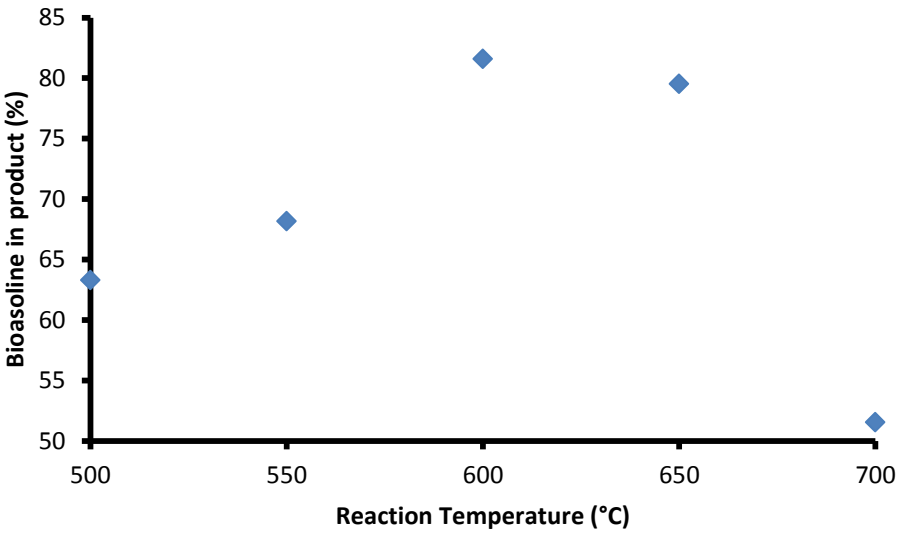

Figure 4.14: Change in bio-gasoline with reaction temperature

The trend observed in the graph is expected for thermal cracking as it is a high temperature which is the dominant reason for cracking (Bridgwater and Peacocke, 2000). The drop in biogasoline product is as a result of extensive cracking of the oil to lower hydrocarbon chain lengths which fall beneath the gasoline carbon chain length. This extensive cracking comes as a result of the elevated temperatures. Less oil was collected in the flask at higher temperatures as more gas and char were produced.

4.4 Hydrocracking

4.4.1 Catalyst calcination temperature variation

The catalyst calcination temperature was varied whilst the reaction temperature (210°C), reaction time (1hr), hydrogen gas pressure (0.5kPa) and catalyst/oil ratio (1/75) were kept constant. The highest biogasoline production was recorded for the catalyst which was calcined at 700°C with a product of 75.7%. All other temperatures were lower than 700°C and produced similar amounts of biogasoline as shown in figure 4.15.

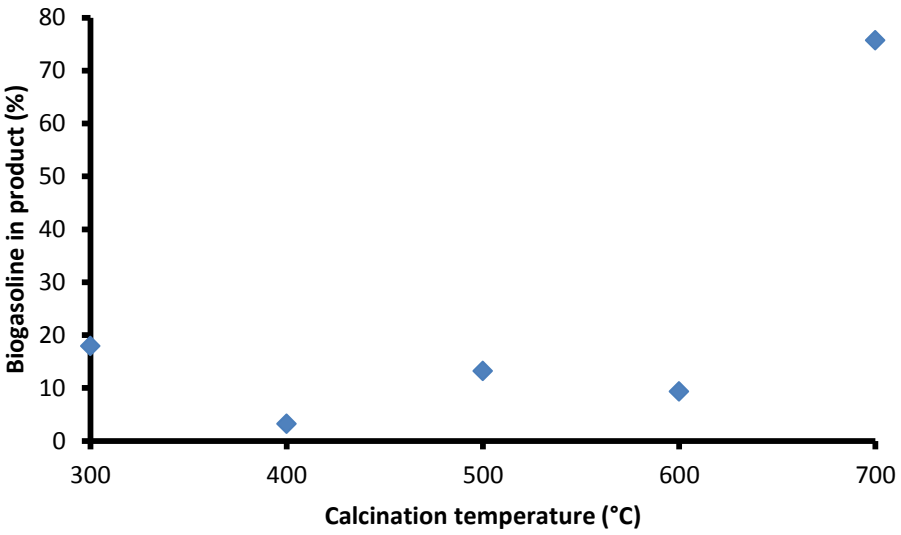

Figure 4.15: Bio-gasoline change with calcination temperature

This trend is to be expected as highlighted by literature and supported by catalyst characterization results, the higher the calcination temperature, the higher the catalyst activity. From these results, 700°C is the minimum temperature the catalyst should be calcined as there is a major increase in production from 600°C. It is important to note that although the highest calcination temperature yields the best results, going any higher might lead to major catalyst deactivation through sintering. In addition, the melting point of the catalyst has to be taken into consideration which is 900°C.

4.4.2 Oil/catalyst ratio variation

The catalyst/oil ratio was varied with reaction temperature (210°C), reaction time (1hr) and catalyst calcination temperature (700°C) kept constant. The amount of biogasoline in the product was highest at the ratio suggested by Mohammad Nasikin et al., (2009) with a value of 75.7%. All other catalyst variations produced low yields all falling between 10% and 14% as shown in figure 4.16.

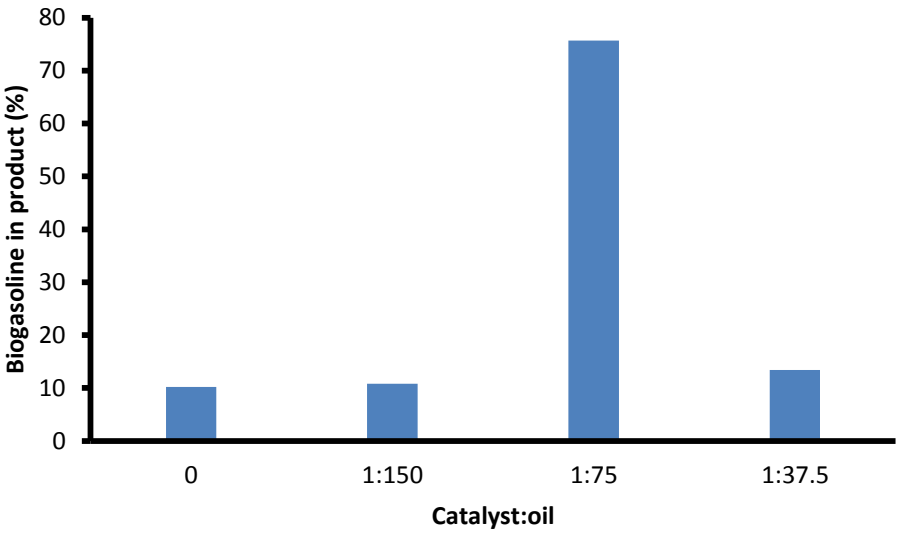

Figure 4.16: Bio-gasoline change with catalyst ratio

This trend can be attributed to the fact that the amount of catalyst used plays a role in the extent of cracking. Too little catalyst could lead to low levels of cracking of the long hydrocarbon chain rich oil. On the other hand, too much catalyst could lead to high levels of cracking due to the greater availability of active sites for the reactions to take place. This leads to low hydrocarbon chain lengths which fall below the gasoline range favoured.

4.4.3 Reaction temperature variation

The reaction temperature was varied while keeping the hydrogen pressure (0.5kPa), reaction time (1hr), catalyst/oil ratio (1/75) and catalyst calcination temperature (700°C) constant. Results in the figure below show that there is a steady increase in biogasoline production with an increase in reaction temperature within the temperature range used.

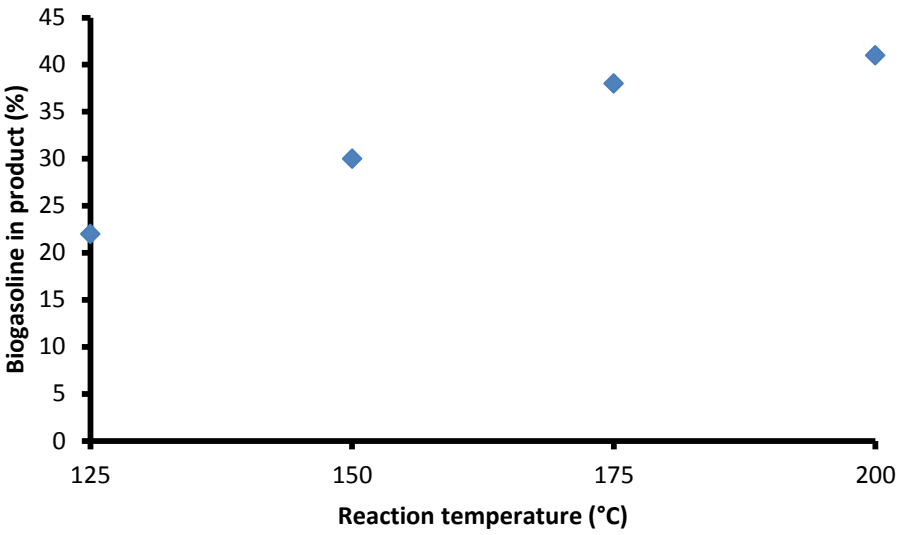

Figure 4.17: Bio-gasoline change with reaction temperature

This trend is to be expected given that temperature is a key parameter in the cracking of long chain hydrocarbons as also observed under thermal cracking. While it is preferred to have an increase in biogasoline yield, a trade off needs to be made given that increasing reaction temperature will lead to an increase in operation costs. As a result lower temperatures tend to be preferred.

4.4.4 Reaction time variation

Reaction time was varied while holding the other four parameters constant; hydrogen pressure (0.5kPa), catalyst/oil ratio (1/75), reaction temperature (210°C) and catalyst calcination temperature (700°C). Generally, an increase in reaction time leads to an increase in biogasoline production as shown in figure 4.18.

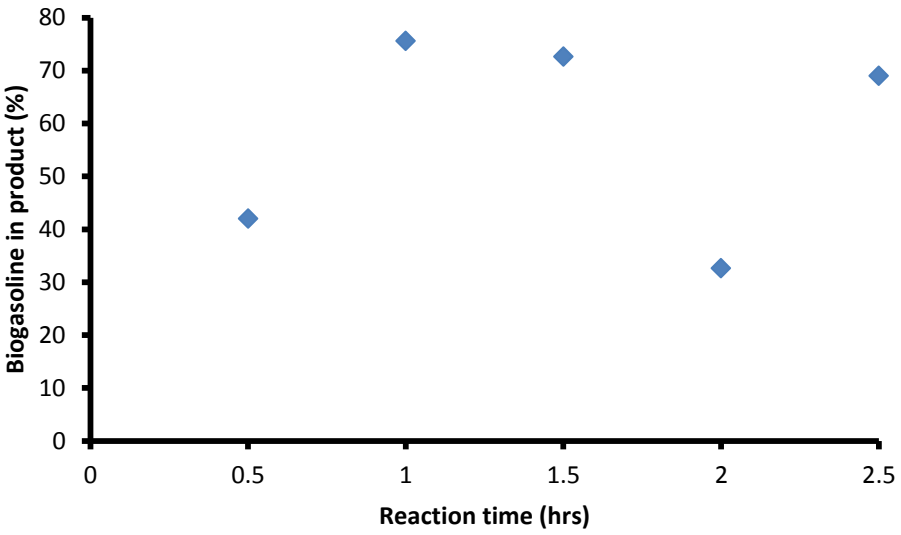

Figure 4.18: Bio-gasoline change with reaction time

There is an increase in production with time before it levels out. Taking into consideration all results, the point at 2hrs can be considered as an outlier. The reactants from the flask require a certain amount of time to react together and from the results, a reaction time of 1hr is the optimum time.

4.5 Thermal cracking and hydrocracking comparison

Due to the variation in conditions between thermal cracking and hydrocracking, not a lot of the results can be picked out for direct comparison. However, the effect of the catalyst on the two systems can be effectively compared on a run to run basis. From figure 4.19 it can be seen that although thermal cracking produced the highest amount of biogasoline (attributed in earlier section as due to elevated temperatures) hydrocracking at the suggested literature ratio produced the highest biogasoline.

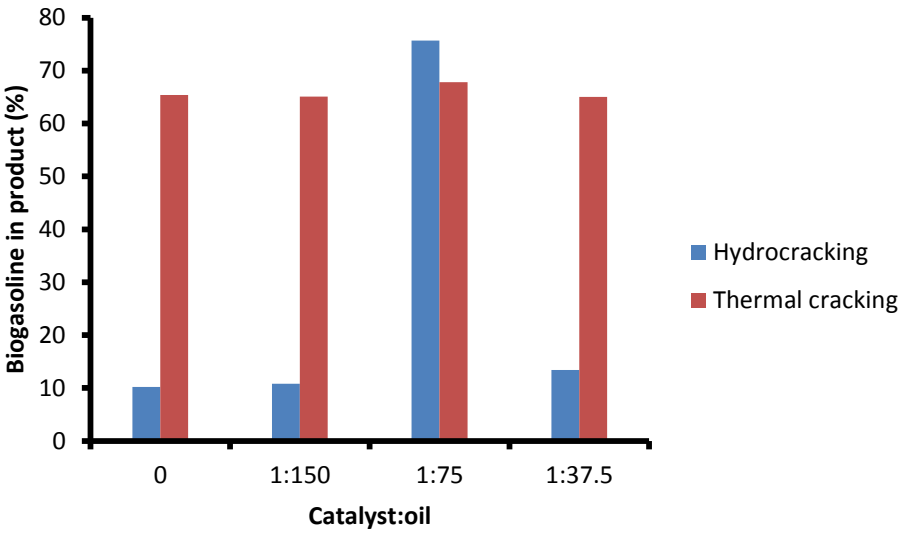

Figure 4.19: Comparison between thermal cracking and hydrocracking

It can be concluded that the catalyst is more suited for hydrocracking given its higher performance in the system.

Both systems recorded higher biogasoline production with an increase in temperature with thermal cracking peaking and then dropping. It is important to note however that hydrocracking managed to produce biogasoline at lower temperatures than thermal cracking.

There was no specific trend observed on the effect of varying calcination temperature in thermal cracking system as shown in the results in section 6.3.1 whereas for hydrocracking, catalyst performance was distinctly high at elevated calcination temperatures.

The identity and nature (carbon chain length and elemental composition) of the product biogasoline was similar in both systems. For the array of compounds present please refer to appendix A.

4.6 Sulphur content of produced biogasoline

Sulphur is used as an indicator of how clean a fuel is. The amount of sulphur contained in the produced biogasoline was calculated in percentage and is presented in tables below.

Table 4.3: Sulphur content in products for thermal cracking

Calcination Temperature (°C)	**Sulphur containing in produced biogasoline**
300	700 ppm
400	1,100 ppm
500	± 0 ppm
600	1,600 ppm
700	3,300 ppm
Reaction Temperature (°C)	**% Sulphur containing in produced biogasoline**
500	1,100 ppm
550	400 ppm
600	6,100 ppm
650	300 ppm
700	13,000 ppm
Catalyst Quantity	**% Sulphur containing in produced biogasoline**
None	27,000 ppm
Half literature value	± 0 ppm
Literature value	9,000 ppm
Double literature value	7,020 ppm

Table 4.4: Sulphur content in products for hydrocracking

Hydrocracking	
Calcination Temperature (°C)	**Sulphur containing compounds**
300	73,700 ppm
400	9,900 ppm
500	46,200 ppm
600	56,200 ppm
700	5,900 ppm
Reaction Temperature (°C)	**Sulphur containing compounds**
125	14,200 ppm
150	15,800 ppm
175	± 0 ppm
200	74,100 ppm
Catalyst Quantity	**% Sulphur containing compounds**
None	8,100 ppm
Half literature value	49,000 ppm
Literature value	5,900 ppm
Double literature value	71,500 ppm
Reaction Time (hrs)	**Sulphur containing compounds**
0.5	51,200 ppm
1	5,900 ppm
1.5	± 0 ppm
2	36,800 ppm
2.5	± 0 ppm

The initial percentage of sulphur containing compounds in the waste cooking oil was a low 4,900 ppm. This is in line with the expectations from literature as outlined that biofuels are expected to contain low sulphur levels. From the results above, it can be seen that there is no trend in the reduction or increase of sulphur containing compounds for all the variables in both hydrocracking and thermal cracking runs. It can be concluded however that the sulphur content remains low with the highest sulphur content being 74,100 ppm for hydrocracking

and 90,000 ppm for thermal cracking. Due to the nature of the reactions taking place in the cracking of hydrocarbons, it is possible to notice an increase in the number of sulphur containing compounds as sulphur from cracked molecules of waste cooking oil could joint other molecules which previously did not contain sulphur. A list of identifying compounds containing sulphur refer to appendix A.

4.7 Production comparison to literature

As mentioned in previous sections, the most common biogasoline production process is hydrocracking. The average biogasoline produced in the hydrocracking runs is compared to others in literature Table 4.5.

Table 4.5: Hydrocracking comparison to literature

Feedstock	**Catalyst**	**Bio-gasoline Yield (%)**	**Author**
Fresh cooking oil	Commercial catalyst	10	(Bezergianni et al., 2009)
Used cooking oil	Commercial catalyst	8	(Bezergianni and Kalogianni, 2009)
Calophyllum inophyllum oil	Co-Mo/γ-Al_2O_3	25.6	(Rasyid et al., 2015)
Calophyllum inophyllum oil	Co-Mo/SiO_2	1.11	(Rasyid et al., 2015)
Calophyllum inophyllum oil	Co-Mo/γ-Al_2O_3-SiO_2	-	(Rasyid et al., 2015)
Vacuum gas oil	β+ASA/Ni-Mo	23.4	(Ali et al., 2002)
Used cooking oil	**Synthesized Co-Mo/γ-Al_2O_3**	**75.7**	**This study**

The table shows that the average produced in this study is higher and in addition this is with waste cooking oil. Assuming that the best result from the hydrocracking runs is reproducible, the results are even better with a biogasoline production of 75.7%.

Chapter 5: Conclusions and Recommendations

5.1 Conclusions

Nano-Cobalt Molybdenum catalyst was successfully synthesised using gamma aluminium oxide powder and a solution of cobalt and molybdenum salts. The optimum performing catalyst was calcined at 700°C and had a catalyst pore size of 7.84nm. SEM images confirmed the presence of nano-sized particles existing together with larger micro-sized particles.

Waste cooking oil for the biogasoline production was successfully pre-treated for salt removal with a drop from 13.18% to 4.37% being noted. Solids from the frying process in the restaurant where it was obtained were also successfully removed.

Two production processes were performed, thermal cracking and hydrocracking both managed to yield biogasoline. Effect of catalyst performance on thermal cracking proved to be minimal with temperature being the major factor in cracking. Highest percentage biogasoline achieved under thermal cracking was 81.6% at a reaction temperature of 600°C, catalyst calcination temperature of 700°C and catalyst/oil mass ratio of 1/75. The catalyst performed better under hydrocracking with effects of changes in catalyst calcination temperature and catalyst/oil ratio being more apparent as opposed to thermal cracking. The highest percentage biogasoline in product achieved was 75.7% at a reaction temperature of 210°C, catalyst calcination of 700°C, catalyst/oil mass ratio of 1/75 and reaction time of 1hr. In addition, the catalyst used and method used produced a higher percentage of biogasoline compared to other literature values. The biogasoline produced had low sulphur content with the highest sulphur containing product for hydrocracking having 7.4% and for thermal cracking having 1.3%.

5.2. Recommendations

It is recommended that for hydrocracking, the process be tested at higher temperatures as this could lead to higher yields of bio-gasoline. In addition the hydrocracking can be carried out in gas phase at higher hydrogen partial pressures. Gas phase reactions are known to have

higher conversions given that there is better mass transfer in gaseous phase. This will however require more sophisticated equipment which can handle the higher pressures and temperatures. In addition, the two systems, thermal cracking and hydrocracking could be put in series with one acting as a precursor to the other as is commonly done in industry for various cracking applications.

The catalyst – oil ratio between 1:50 to 1:150 and the calcination temperature between 600 and 800 should be investigated for the optimum findings.

The catalyst can also be trialled with different raw material such as palm kernel oil. The catalyst could be better suited for these types of oil as compared to the waste cooking oil. Furthermore, the aluminium powder used as catalyst support can be screened using specialised sieves in order to concentrate nanoparticle material. This would increase the surface area of the catalyst and potentially lead to greater yields given the rise in reaction rates. Other catalyst preparation techniques such as spray pyrolysis can also be done as an alternative to impregnation which was used in this study. It is important to note that the liquid product still needs to go under distillation to further quantify how much bio-gasoline is produced. Further analysis such as physical property tests such as viscosity measurements can also be done to further ascertain the quality of the bio-gasoline.

References

Aakko-Saksa, P., Koponen, P., Kihlman, J., 2011. Biogasoline options for conventional spark-ignition cars, 1st ed. VTT Technical Research Centre of Finland.

Agarwal, A.K., 2007. Biofuels (alcohols and biodiesel) applications as fuels for internal combustion engines. Progress in Energy and Combustion Science 33, 233–271.

Al-Fatesh, A.S.A., Fakeeha, A.H., 2012. Effects of calcination and activation temperature on dry reforming catalysts. Journal of Saudi Chemical Society 16, 55–61.

Ali, M.A., Tatsumi, T., Masuda, T., 2002. Development of heavy oil hydrocracking catalysts using amorphous silica-alumina and zeolites as catalyst supports. Applied Catalysis A: General 233, 77–90.

Bezergianni, S., Kalogianni, A., 2009. Hydrocracking of used cooking oil for biofuels production. Bioresource Technology 100, 3927–3932.

Bezergianni, S., Voutetakis, S., Kalogianni, A., 2009. Catalytic Hydrocracking of Fresh and Used Cooking Oil. Ind. Eng. Chem. Res. 48, 8402–8406.

Botchwey, C., Dalai, A.K., Adjaye, J., 2004. Kinetics of bitumen-derived gas oil upgrading using a commercial NiMo/Al2O3 catalyst. Canadian Journal of Chemical Engineering 82, 478–487.

Bridgwater, A.V., Peacocke, G.V.C., 2000. Fast pyrolysis processes for biomass. Renewable and Sustainable Energy Reviews 4, 1–73.

Cerqueira Leite, R.C. de, Verde Leal, M.R.L., Barbosa Cortez, L.A., Griffin, W.M., Gaya Scandiffio, M.I., 2009. Can Brazil replace 5% of the 2025 gasoline world demand with ethanol? Energy, 4th Dubrovnik Conference4th Dubrovnik conference on Sustainable Development of energy, Water & Environment 34, 655–661.

Choi, K.-H., Korai, Y., Mochida, I., 2004. Preparation and characterization of nano-sized CoMo/Al2O3 catalyst for hydrodesulfurization. Applied Catalysis A: General 260, 229–236.

Demirbas, A., 2009. Political, economic and environmental impacts of biofuels: A review. Applied Energy, Bio-fuels in Asia 86, Supplement 1, S108–S117.

Deublein, D., Steinhauser, A., 2011. Biogas from Waste and Renewable Resources: An Introduction. John Wiley & Sons.

Dufey, A., 2006. Biofuels Production, Trade and Sustainable Development: Emerging Issues. IIED.

Escobar, J.C., Lora, E.S., Venturini, O.J., Yáñez, E.E., Castillo, E.F., Almazan, O., 2009. Biofuels: Environment, technology and food security. Renewable and Sustainable Energy Reviews 13, 1275–1287.

Forzatti, P., Lietti, L., 1999. Catalyst deactivation. Catalysis Today 52, 165–181.

Gaber, A., Abdel-Rahim, M.., Abdel-Latief, A.Y., 2016. Influence of Calcination Temperature on the Structure and Porosity of Nanocrystalline SnO2 Synthesized by a Conventional Precipitation method. International Journal of Electrochemical Science 11.

Government of Canada, E.C., n.d. ETC Spills Technology Databases, Oil Properties Database [WWW Document]. URL http://www.etc-cte.ec.gc.ca/databases/Oilproperties/ (accessed 2.18.16).

Gray, K.A., Zhao, L., Emptage, M., 2006. Bioethanol. Current Opinion in Chemical Biology, Bioinorganic chemistry / Biocatalysis and biotransformation 10, 141–146.

Greene, D.L., Hopson, J.L., Li, J., 2006. Have we run out of oil yet? Oil peaking analysis from an optimist's perspective. Energy Policy, Hong Kong Editorial Board meeting presentations Hong Kong Editorial Board meeting presentations 34, 515–531.

Greensfelder, B.S., Voge, H.H., Good, G.M., 1949. Catalytic and Thermal Cracking of Pure Hydrocarbons: Mechanisms of Reaction. Ind. Eng. Chem. 41, 2573–2584.

Hassan, S.N., Sani, Y.M., Abdul Aziz, A.R., Sulaiman, N.M.N., Daud, W.M.A.W., 2015. Biogasoline: An out-of-the-box solution to the food-for-fuel and land-use competitions. Energy Conversion and Management 89, 349–367.

Holmgren, J., Marker, T., Petri, J., 2007. Opportunities for Biorenewables. Hydrocarbon Engineering.

Huber, G., Corma, A., Iborra, S., 2006. Synthesis of transportation fuels from biomass: Chemistry, catalyst and engineering. Chem Rev 4044–4098.

Lantelme, F., Groult, H., 2013. Molten Salts Chemistry: From Lab to Applications. Newnes.

Leach, B.E., 1983. Applied industrial catalysis. Academic Press.

Lior, N., 2008. Energy resources and use: The present situation and possible paths to the future. Energy, PRES 2006. 9th Conference of Process Integration, Modelling and Optimisation for Energy Saving and Pollution Reduction - PRES 2006PRES 2006 33, 842–857.

Maugeri, L., 2004. Oil: Never cry wolf - Why the petroleum age is far from over. Science 304, 1114–1115.

McMillan, J.D., 1997. Bioethanol production: Status and prospects. Renewable Energy, World Renewable Energy Congress IV Renewable Energy, Energy Efficiency and the Environment 10, 295–302.

Mohammad Nasikin, Susanto, B., Hirsaman, M., 2009. Biogasoline from Palm Oil by Simultaneous Cracking and Hydrogenation Reaction over Nimo/zeolite Catalyst. World Applied Sciences Journal 75–79.

Mohanty, S., Kunzru, D., Saraf, D.N., 1990. Hydrocracking: a review. Fuel 69, 1467–1473.

Niven, R.K., 2005. Ethanol in gasoline: environmental impacts and sustainability review article. Renewable and Sustainable Energy Reviews 9, 535–555.

Phan, A.N., Phan, T.M., 2008. Biodiesel production from waste cooking oils. Fuel 87, 3490–3496.

Rasyid, R., Prihartantyo, A., Mahfud, M., Roesyadi, A., 2015. Hydrocracking of Calophyllum inophyllum Oil With Non-sulfide CoMo Catalysts. Bull. Chem. React. Eng. Catal. 10, 61–69.

Roberts, 2008. Chemical Reactions and Chemical Reactors, 1 edition. ed. Wiley, Hoboken, NJ.

Rosillo-Calle, F., Johnson, F.X., 2010. Food versus Fuel : An informed introduction to biofuels. Zed Books.

Sadrameli, S.M., 2015. Thermal/catalytic cracking of hydrocarbons for the production of olefins: A state-of-the-art review I: Thermal cracking review. Fuel 140, 102–115.

Shafiee, S., Topal, E., 2009. When will fossil fuel reserves be diminished? Energy Policy 37, 181–189.

Timilsina, G.R., Mevel, S., 2012. Biofuels and Climate Change Mitigation: A CGE Analysis Incorporating Land-Use Change. Environ Resource Econ 55, 1–19.

Tiwari, R., Rana, B.S., Kumar, R., Verma, D., Kumar, R., Joshi, R.K., Garg, M.O., Sinha, A.K., 2011. Hydrotreating and hydrocracking catalysts for processing of waste soya-oil and refinery-oil mixtures. Catalysis Communications 12, 559–562.

U.S Department of Energy, 2015a. Alternative Fuels Data Center: Renewable Natural Gas (Biomethane) Production http://www.afdc.energy.gov/fuels/natural_gas_renewable.html (accessed 2.23.16).

U.S Department of Energy, 2015b. Alternative Fuels Data Center: Ethanol http://www.afdc.energy.gov/fuels/ethanol.html (accessed 2.23.16).

U.S Department of Energy, 2014. Alternative Fuels Data Center: Biodiesel Production and Distribution. http://www.afdc.energy.gov/fuels/biodiesel_production.html (accessed 2.23.16).

Vassiliou, M.S., 2009. Historical Dictionary of the Petroleum Industry. Scarecrow Press.

Weiland, P., 2009. Biogas production: current state and perspectives. Appl Microbiol Biotechnol 85, 849–860.

Xiong, H., Zhang, Y., Wang, S., Li, J., 2005. Fischer–Tropsch synthesis: the effect of Al2O3 porosity on the performance of Co/Al2O3 catalyst. Catalysis Communications 6, 512–516.

Zhang, Y., Dubé, M.A., McLean, D.D., Kates, M., 2003. Biodiesel production from waste cooking oil: 1. Process design and technological assessment. Bioresource Technology 89, 1–16.

Appendix A: Raw Data

Table A.1: ICP-OES Concentration Results

Sample	Co	Mo	Al
	ppm	ppm	ppm
Calcined 300°C	136.8	236.25	3476.25
Calcined 400°C	143.4	236.85	5449.5
Calcined 500°C	17.34	27.72	778.5
Calcined 600°C	6474	10626	nd
Calcined 700°C	85.8	139.6	3579
1:1	6474	10626	nd
1:2	8685	28800	3036
1:3	72.36	390	nd
2:1	17991	15714	nd
3:1	30300	19395	< -558.076

Table A.2: Sulphur containing compounds after cracking

Formula	Name
C8H10O2S	Ethyl 2-thiopheneacetate
C6H4O3S	Thiophene-2-carboxylic acid, 5-formyl-
C5H9NOS	6-Methyltetrahydro-1,3-oxazine-2-thione
C8H20O2SSi2	Mercaptoacetic acid, 2TMS derivative
C8H22OSSi2	Mercaptoethanol, 2TMS derivative

Table A.3: Biogasoline compounds in thermal cracking and hydrocracking

Formula	Name
C9H12	Benzene, 1-ethyl-2-methyl-
C11H20	Z-1,6-Undecadiene
C6H6O	Phenol
C9H14	Spiro[4.4]non-1-ene
C10H20	1-Decene
C10H22	Decane
C9H12	Benzene, 1,2,3-trimethyl-
C9H10	Benzene, 1-ethenyl-2-methyl-
C10H20	2-Decene, (Z)-
C9H10	Benzene, 2-propenyl-

C10H18	5-Decyne
C8H12	3-(2-Propenyl)cyclopentene
C9H10	Indane
C10H18	Cyclopentene, 1-pentyl-
C9H8	1-Propyne, 3-phenyl-
C10H14	Benzene, n-butyl-
C10H14	Benzene, 1-methyl-4-propyl-
C12H24O	2-Dodecanone
C10H20O2	2-Nonanone, 3-(hydroxymethyl)-
C12H24	Cyclopropane, 1-methyl-2-octyl-
C11H24	Undecane
C11H22	2-Undecene, (Z)-
C9H18O	Nonanal
C11H22	4-Undecene, (E)-
C7H14O2	Heptanoic acid
C11H20	1,4-Undecadiene, (E)-
C7H14O2	Heptanoic acid
C7H14O2	Heptanoic acid
C7H8O	7-Oxabicyclo[2.2.1]hept-2-ene, 5-methylene-
C10H12	Benzene, 2-ethenyl-1,4-dimethyl-
C7H10	1-Methylcyclohexa-1,3-diene
C8H14	2,4-Octadiene
C11H20	Cyclohexene, 3-pentyl-
C10H12	Benzene, 4-ethenyl-1,2-dimethyl-
C10H10	1H-Indene, 3-methyl-
C11H16	Benzene, pentyl-
C11H18	5-Pentylcyclohexa-1,3-diene
C9H16	1-Methylbicyclo[3.2.1]octane
C10H10	1H-Indene, 3-methyl-
C10H12O	Ether, p-methylbenzyl vinyl
C10H12	Naphthalene, 1,2,3,4-tetrahydro-
C10H10	Benzene, (1-methylene-2-propenyl)-
C8H16O	2-Heptanone, 5-methyl-
C11H20O2	4-Ethyl-3,7-nonandione
C12H24	6-Dodecene, (E)-
C12H24	1-Dodecene
C9H18O	2-Nonanone
C10H16	D-Limonene
C12H26	Dodecane
C12H24	4-Dodecene
C10H8	1H-Indene, 1-methylene-
C8H16O2	Octanoic acid

C12H22	Z-1,8-Dodecadiene
C12H22	Cyclododecene, (E)-
C12H22O2	Hexanoic acid, 3-hexenyl ester, (Z)-
C8H14	3,4-Octadiene
C12H18	Benzene, (1,3-dimethylbutyl)-
C12H16	Benzene, cyclohexyl-
C12H18	Benzene, hexyl-
C11H12	1H-Indene, 4,7-dimethyl-
C12H18	Benzene, (1,3-dimethylbutyl)-
C11H12	Benzene, (2-cyclopropylethenyl)-
C11H14	Naphthalene, 1,2,3,4-tetrahydro-6-methyl-
C9H18	Cyclooctane, methyl-
C10H20O2	2-Nonanone, 3-(hydroxymethyl)-
C10H16O	2-Cyclopenten-1-one, 2-pentyl-
C9H18O2	Nonanoic acid
C11H10	Naphthalene, 1-methyl-
C11H20	Cycloundecene (Z)
C11H10	Naphthalene, 1-methyl-
C12H16O	Spiro[3.5]nona-5,7-dien-1-one, 5,9,9-trimethyl-
C12H18	Dispiro[2.1.2.4]undecane, 8-methylene-
C12H24O	4-Dodecanone
C12H14	Dicyclopropa[cd,gh]pentalene, octahydro-1-(2-methyl-1-propenylidene)-
C11H24O	1-Undecanol
C10H20O2	n-Decanoic acid
C10H18O2	9-Decenoic acid
C10H18O2	Vinyl caprylate
C12H12	Naphthalene, 2,6-dimethyl-
C10H15N	4-Ethylphenethylamine
C12H12	Benzene, 2,5-cyclohexadien-1-yl-
C12H22	1-Dodecyne
C9H16O	2,6-Nonadien-1-ol
C12H18O	(3-Methylphenyl) methanol, 1-methylpropyl ether
C12H12	Naphthalene, 1,7-dimethyl-
C10H18	Cyclodecene, (Z)-
C11H20O2	Undecylenic acid
C11H18O	2-Cyclopenten-1-one, 2-methyl-3-pentyl-
C12H10	Acenaphthene
C11H18O	Bicyclo[3.1.1]hept-2-ene-2-ethanol, 6,6-dimethyl-
C8H10O2S	Ethyl 2-thiopheneacetate
C10H18	Cyclohexene, 3-(2-methylpropyl)-
C12H24O	Decane, 1-(ethenyloxy)-
C8H14	1,4-Pentadiene, 3-propyl-

C12H18O	1,2-Epoxy-5,9-cyclododecadiene
C9H14O5	2-Hexenedioic acid, 2-methoxy-, dimethyl ester
C8H10N4O2	Caffeine
C10H22	Hexane, 4-ethyl-2,2-dimethyl-
C15H32	Dodecane, 2,7,10-trimethyl-
C20H26	Heptane, 2,6-diphenyl-3-methyl-
C16H26	Benzene, (1-methylnonyl)-
C6H4O3S	Thiophene-2-carboxylic acid, 5-formyl-
C10H18	9-Methylbicyclo[3.3.1]nonane
C10H18	Cyclodecene, (Z)-
C10H20	1R,2c,3t,4t-Tetramethyl-cyclohexane
C11H18	Naphthalene, 1,2,3,4,4a,5,6,7-octahydro-4a-methyl-
C12H18	Benzene, (1-methylpentyl)-
C12H22O	13-Oxabicyclo[10.1.0]tridecane
C8H16	1-Hexene, 5,5-dimethyl-
C12H24O	Z-4-Dodecenol
C11H10	1H-Indene, 1-ethylidene-
C11H20	Cycloundecene (Z)
C11H20	E-1,6-Undecadiene
C7H8	Toluene
C11H20	Cycloundecene (Z)
C11H20	Cycloundecene (Z)
C9H18O	5-Hepten-1-ol, 2,6-dimethyl-
C11H20O2	Oxacyclododecan-2-one
C19H32	Benzene, (1-hexylheptyl)-
C11H22	Cyclopropane, 1-butyl-1-methyl-2-propyl-
C12H21F3O2	Acetic acid, trifluoro-, 3,7-dimethyloctyl ester
C8H14O	9-Oxabicyclo[6.1.0]nonane
C11H20N2	1-(tert-Butyl)-3-cyclohexylcarbodiimide
C9H18O	(6Z)-Nonen-1-ol
C12H17BO2	1,3,2-Dioxaborinane, 2-ethyl-5-methyl-4-phenyl-
C10H18O2	Allyl heptanoate
C12H22O	11-Dodecen-2-one
C10H20O	2-Decanone
C8H8O3	3',5'-Dihydroxyacetophenone
C12H18O	Phenol, 4-hexyl-
C6H12O2	Pentanoic acid, 4-methyl-
C10H20O	2-Decanone

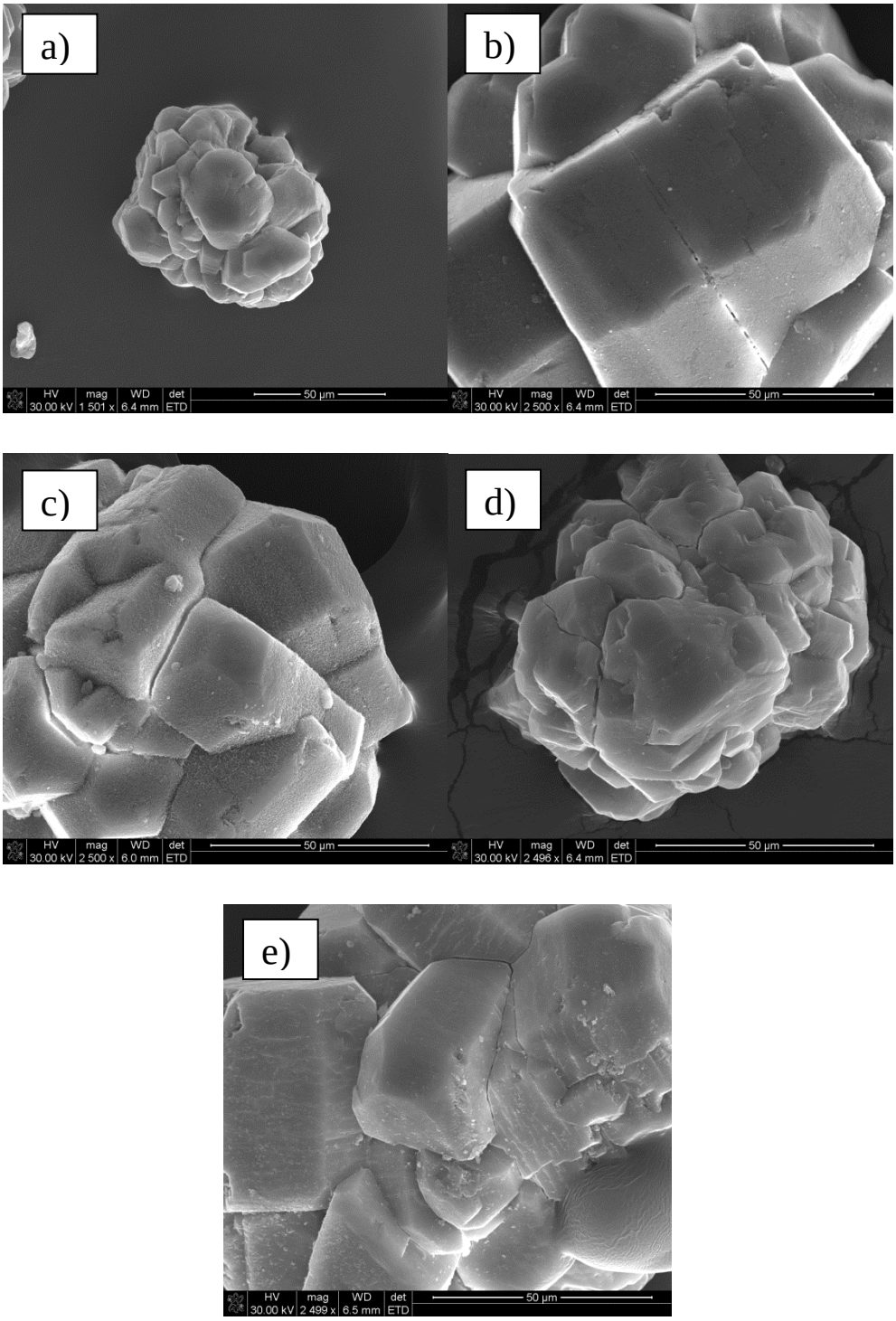

Figure A.1: Low magnification images of $CoMo/Al_2O_3$ for varying calcination temperatures a) 300°C b) 400°C c) 500°C d) 600°C e) 700°C